RELATIVISTIC EFFECTS ON THE ORBITS OF THE CLOSEST STARS TO THE BLACK HOLE AT THE CENTER OF THE GALAXY

EREP 24: 23/07/2024

Karim ABD EL DAYEM

Supervisors: Frédéric VINCENT, Thibaut PAUMARD, Guy PERRIN

LESIA | l'Observatoire de Paris | PSL

CONTEXT & AIMS

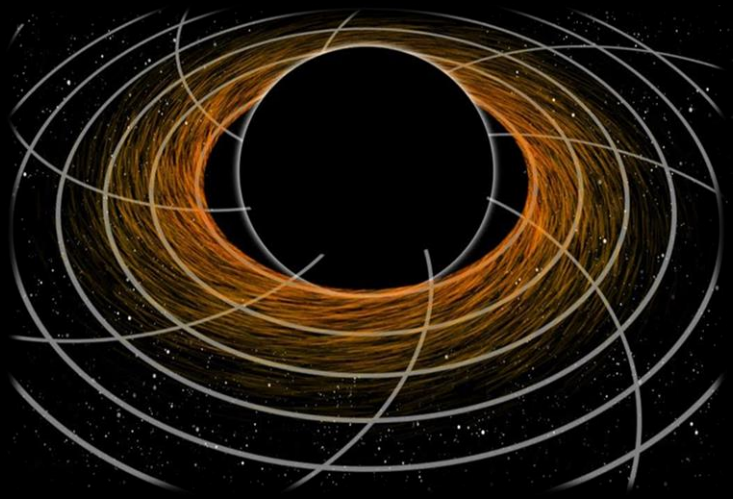

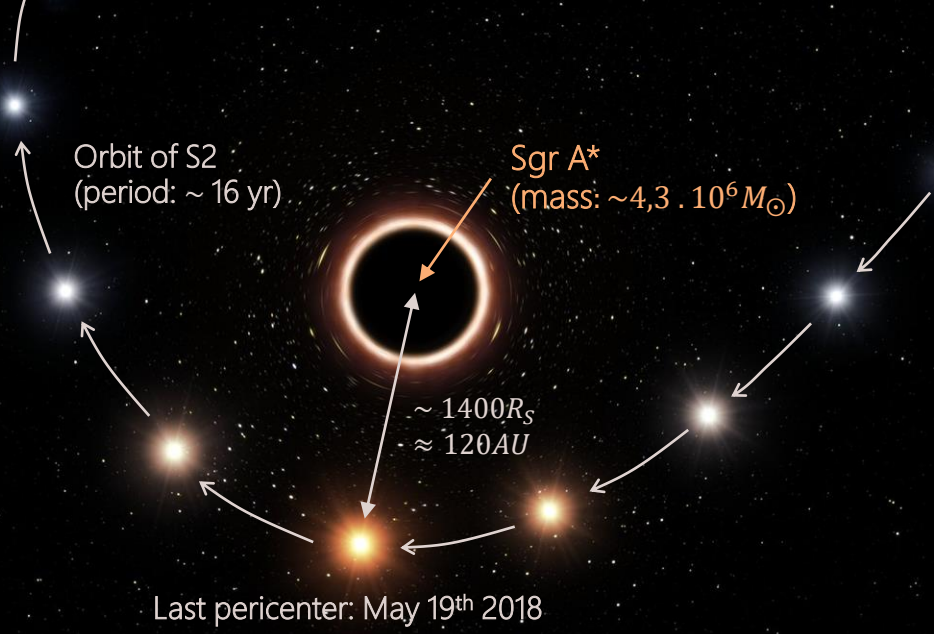

Curved space-time ⟷ Mass

Spinning space-time ⟷ Spin

Oblate space-time ⟷ Quadrupole moment

No hair-theorem:

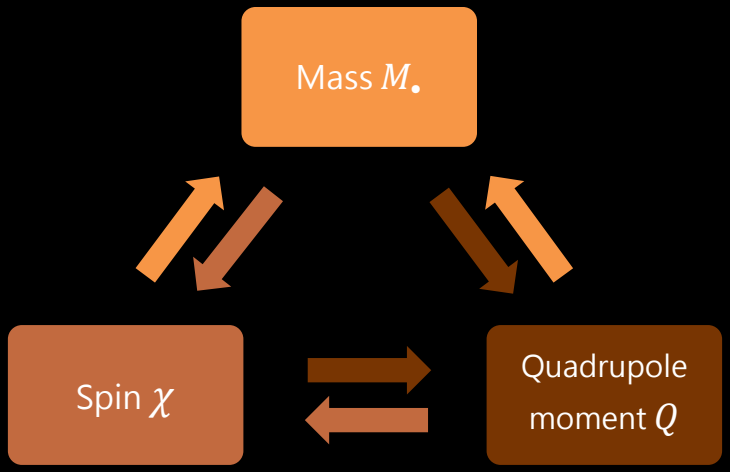

CONTEXT & AIMS

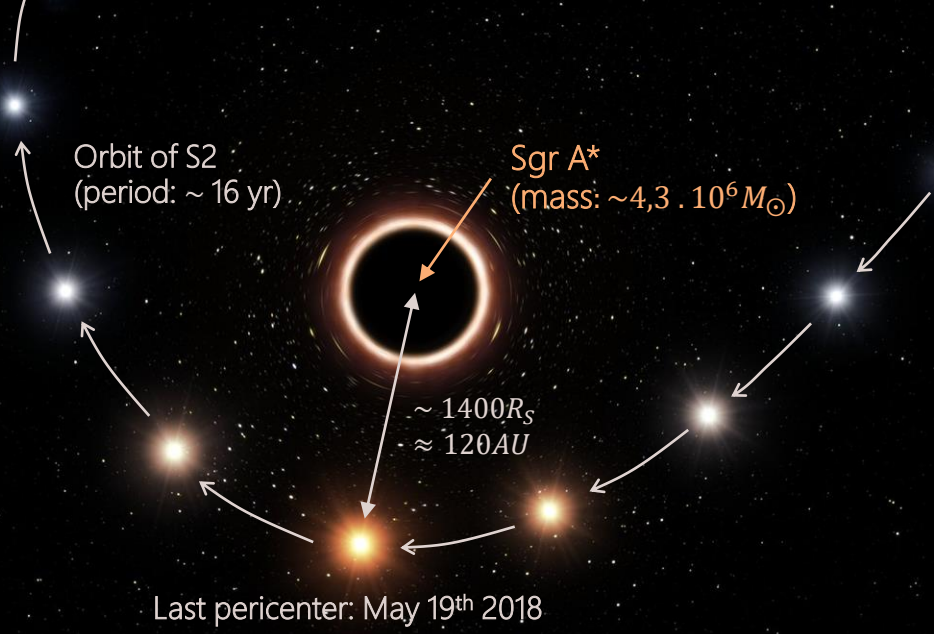

Perturbation to Kepler:

$$a_{2PN} = a_{Sch} + a_\chi + a_Q$$

with:

$$a_\chi \propto \chi$$
$$a_Q \propto Q$$

Independently fitting χ and Q from the monitoring of S-stars

Test the no-hair theorem:

$$Q = -\frac{G^2 M_\bullet^3}{c^4}\chi^2$$

No hair-theorem:

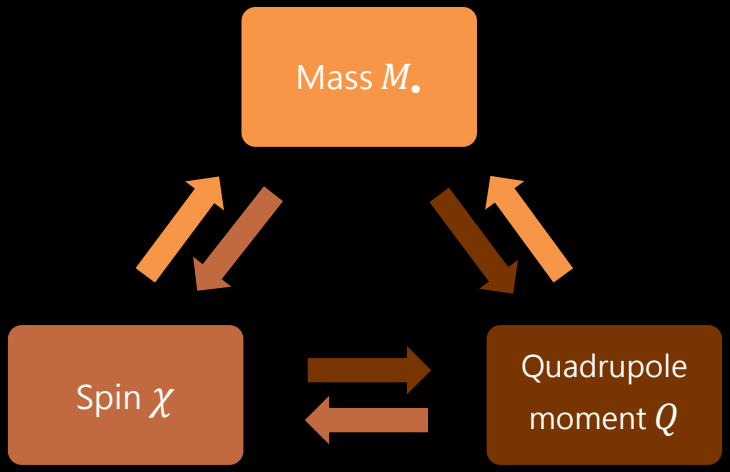

CONTEXT & AIMS

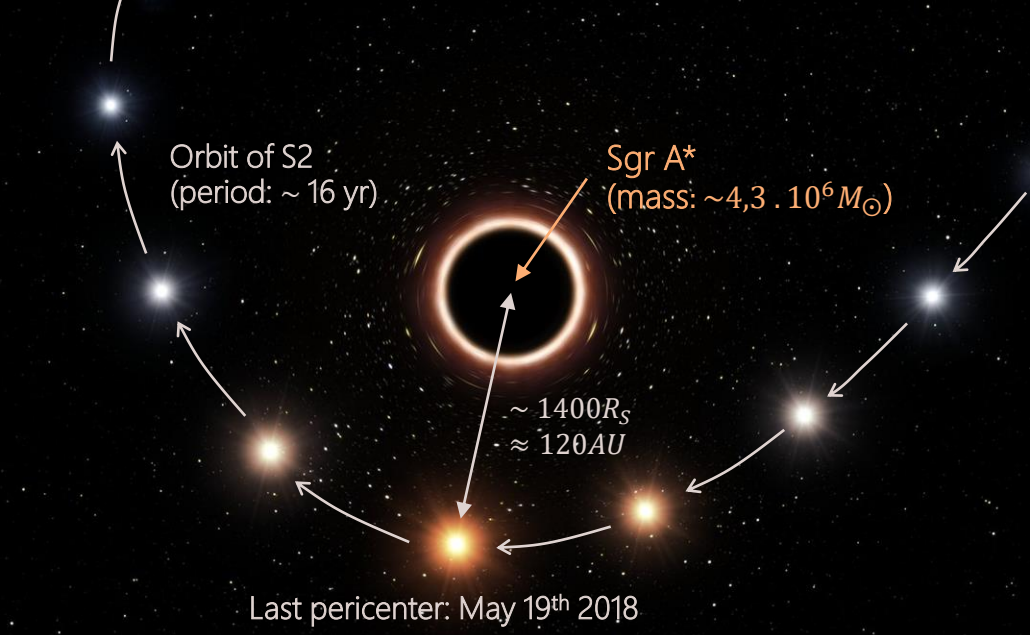

Perturbation to Kepler:

$$a_{2PN} = a_{Sch} + a_\chi + a_Q$$

with:

$$a_\chi \propto \chi$$
$$a_Q \propto Q$$

Independently fitting χ and Q from the monitoring of S-stars

Test the no-hair theorem:

$$Q = -\frac{G^2 M_\bullet^3}{c^4}\chi^2$$

No hair-theorem:

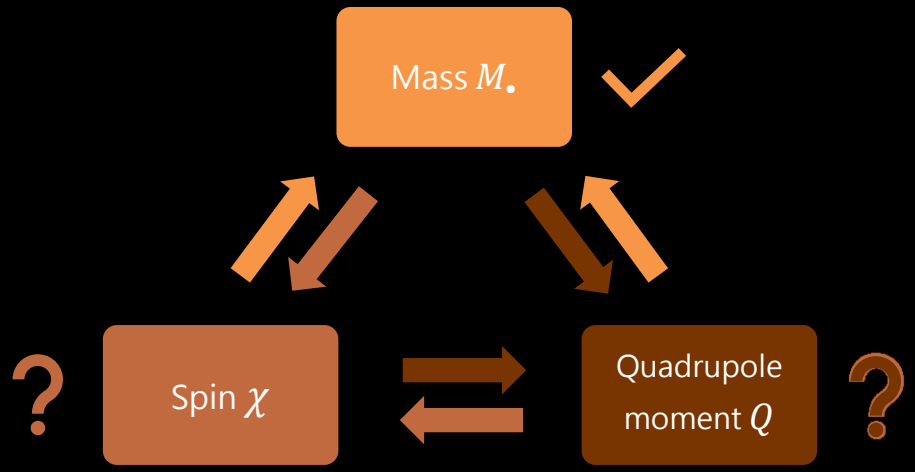

Maximal accuracy	Astrometric (µas)	Spectroscopic (km/s)	State
SINFONI (VLT)	–	≈ 10	Decommissioned
NIRSPEC (Keck)	–	≈ 10	Operational
GRAVITY (VLT)	≈ 10	–	Operational
ERIS (VLT)	–	≈ 10	Operational
GRAVITY+ (VLT)	≈ 10	–	Operational in 2024+
MICADO (E-ELT)	≈ 50	≈ 1	Operational in 2028+

DEPEND ON THE FLUX REACHING THE INSTRUMENT

INSTRUMENTATION

VLT (Paranal) :

- GRAVITY (Interferometer)

$m_K \leq 19$

- SINFONI (Spectrograph)

Maximal accuracy	Astrometric (µas)	Spectroscopic (km/s)	State
SINFONI (VLT)	–	≈ 10	Decommissioned
NIRSPEC (Keck)	–	≈ 10	Operational
GRAVITY (VLT)	≈ 10	–	Operational
ERIS (VLT)	–	≈ 10	Operational
GRAVITY+ (VLT)	≈ 10	–	Operational in 2024+
MICADO (E-ELT)	≈ 50	≈ 1	Operational in 2028+

GRAVITY+ CAN MULTIPLY THE NUMBER OF PHOTONS UP TO A FACTOR 20!

-Better temporal coverage

-Less systematic errors

-Less photon noise

DEPEND ON THE FLUX REACHING THE INSTRUMENT

POSSIBILITY OF DETECTING OTHER STARS

INSTRUMENTATION

VLT (Paranal) :

- GRAVITY → GRAVITY + (Interferometer)

$m_K \leq 19$ → $m_K \leq 22$

- ERIS (Spectrograph)

2nd Year work:
Impact of the relative orientations

Spin parameters:
$(\chi,\ i_{bh},\ \Omega_{bh})$

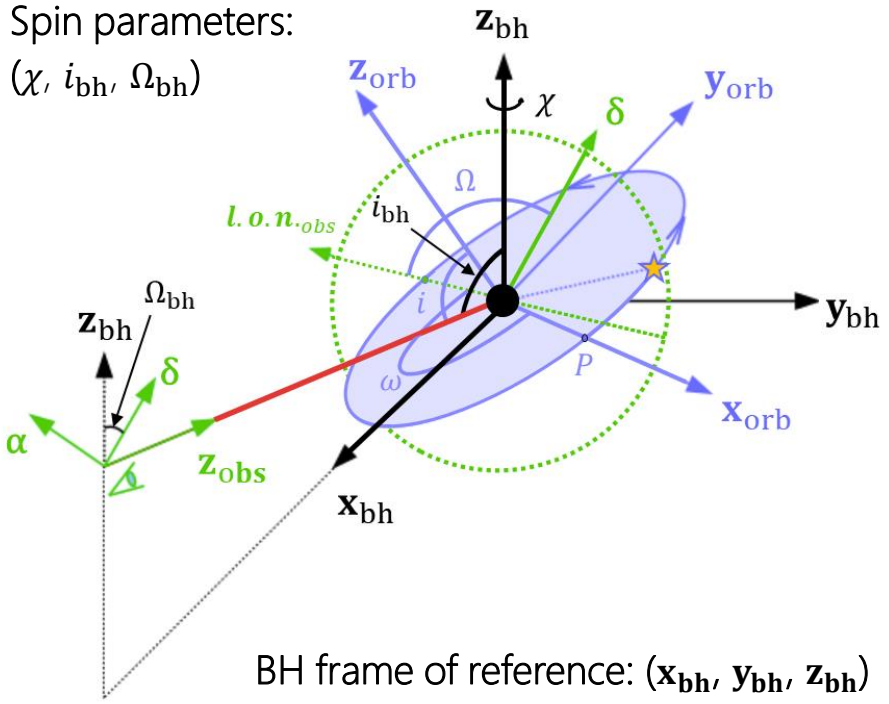

BH frame of reference: $(x_{bh},\ y_{bh},\ z_{bh})$

Orbit frame of reference: $(x_{orb},\ y_{orb},\ z_{orb})$

Observer's frame of reference: $(\alpha,\ \delta,\ z_{obs})$

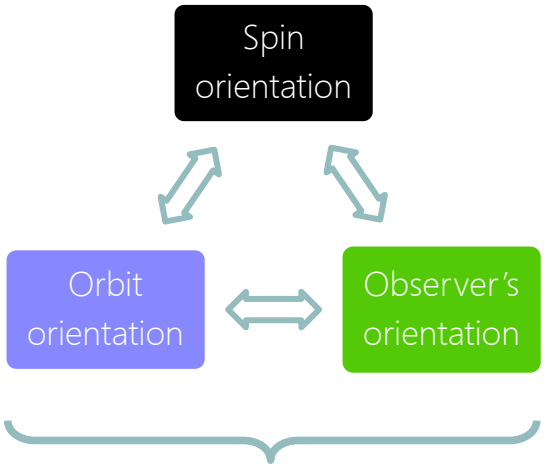

Impact the secular evolution of the pericenter/apocenter

↳ Intuition?

↓

Study the different types of precessions

2nd Year work:
Impact of the relative orientations

Spin parameters:
$(\chi,\ i_{bh},\ \Omega_{bh})$

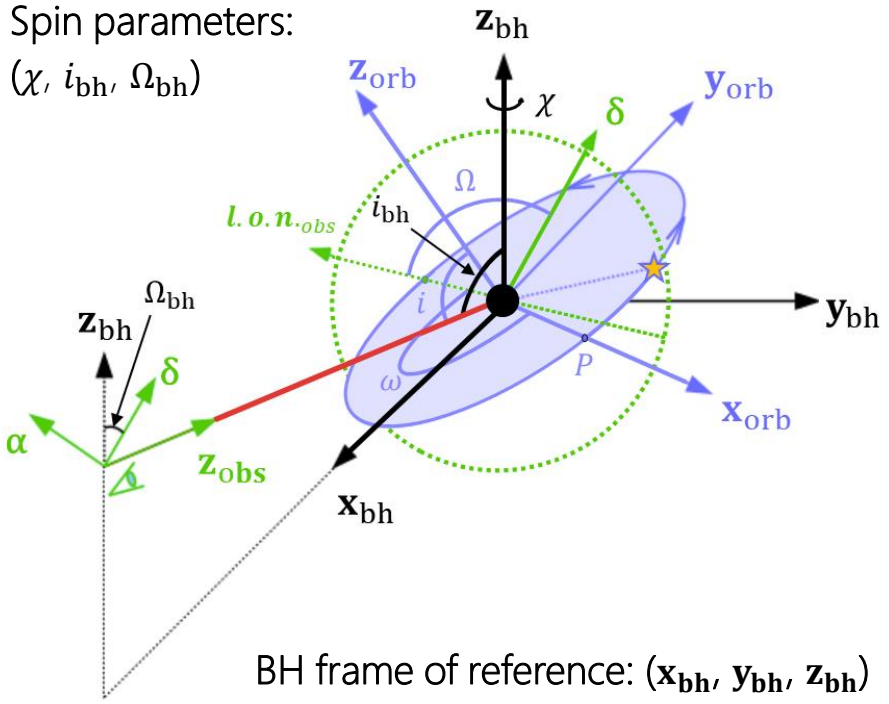

BH frame of reference: $(x_{bh},\ y_{bh},\ z_{bh})$

Orbit frame of reference: $(x_{orb},\ y_{orb},\ z_{orb})$

Observer's frame of reference: $(\alpha,\ \delta,\ z_{obs})$

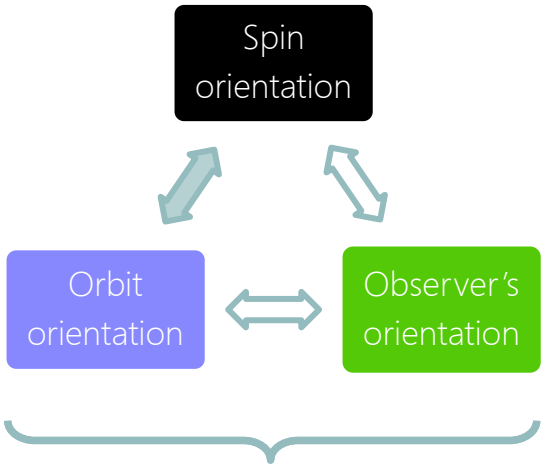

Impact the secular evolution of the pericenter/apocenter

↳ Intuition?

↓

Study the different types of precessions

TOOLS: PALETTE OF RELATIVISTIC MODELS

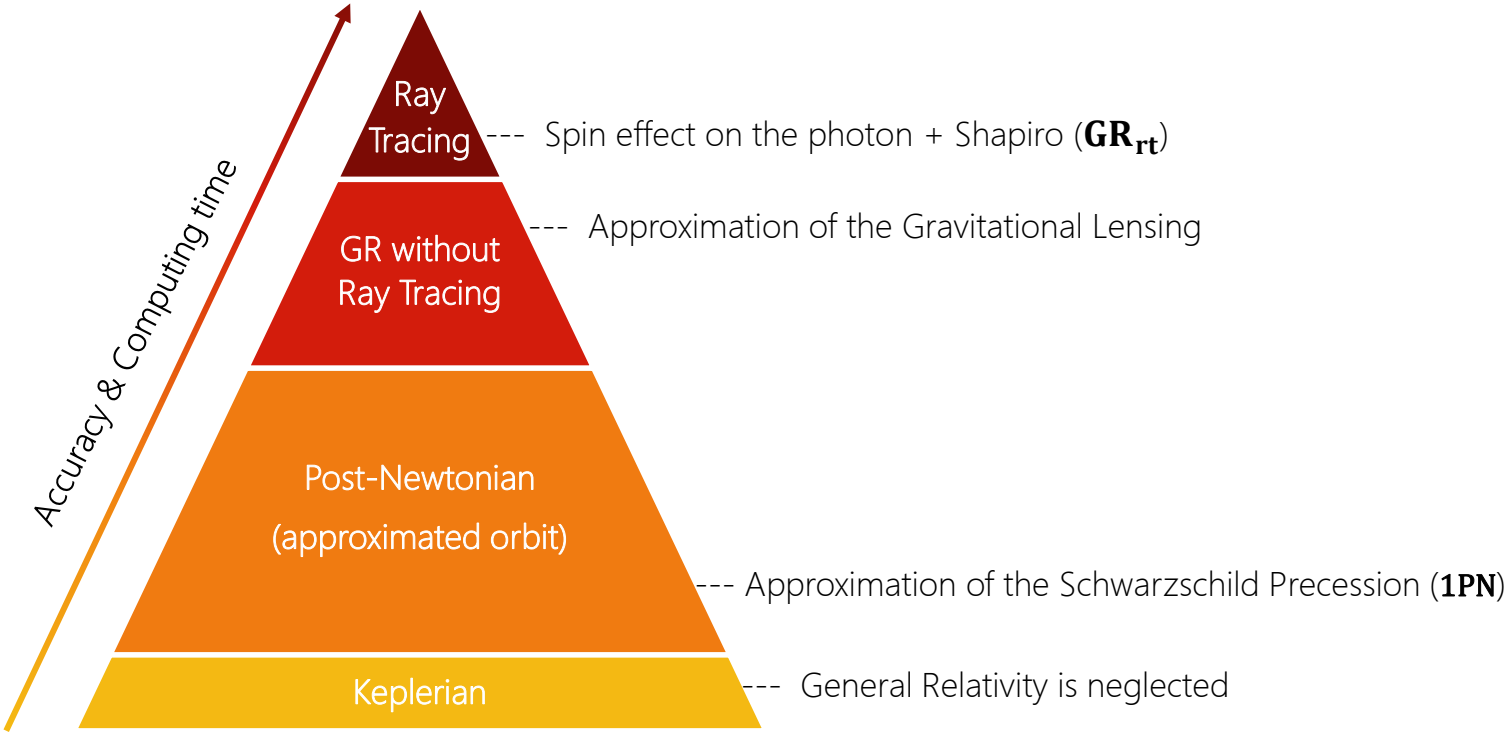

TOOLS: PALETTE OF RELATIVISTIC MODELS

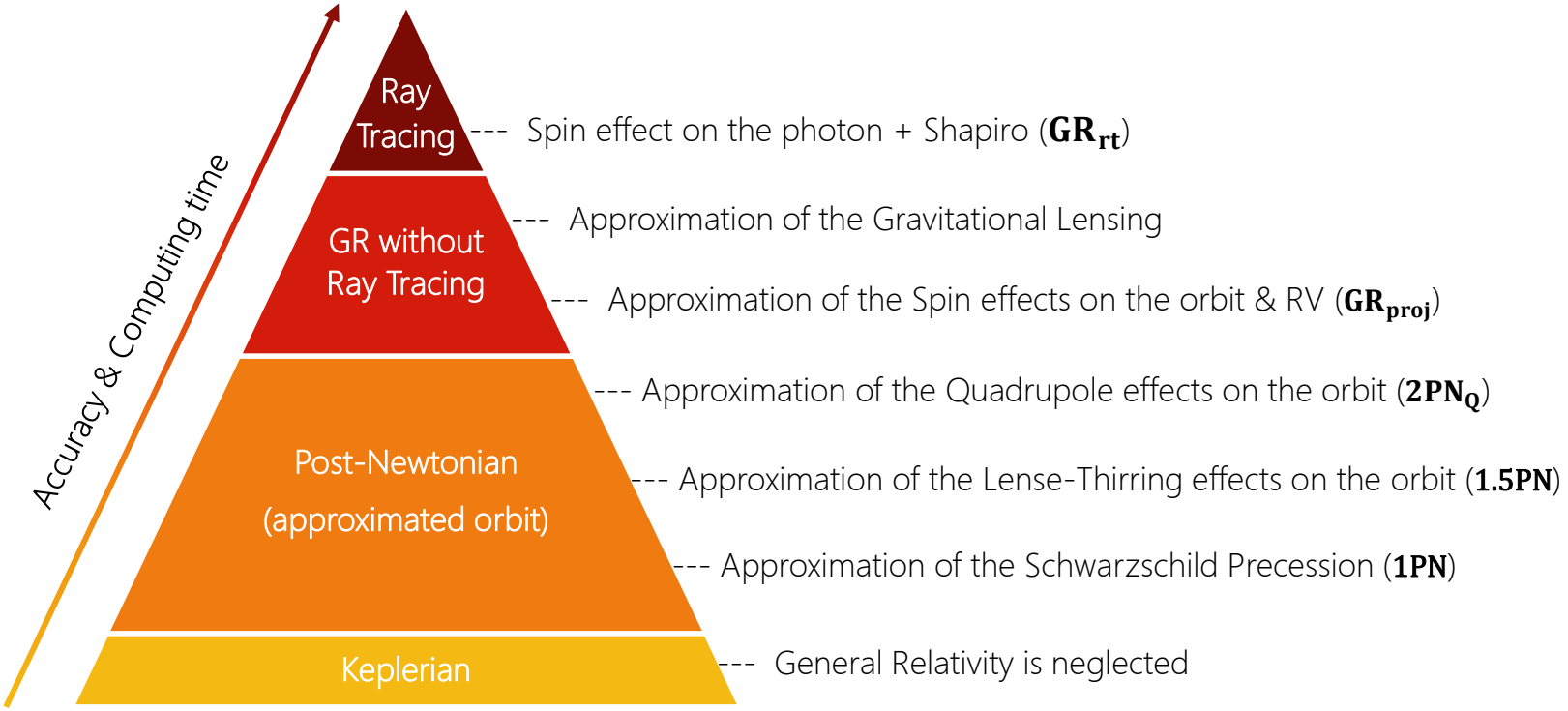

↳ Development of the **1.5PN**, $\mathbf{GR_{proj}}$ and $\mathbf{2PN_Q}$ models

Karim

TOOLS: PALETTE OF RELATIVISTIC MODELS

2PN order for closer-in stars

2PN_sch : Schwarzschild

2PN_LT : Schwarzschild + χ

2PN_Q : Schwarzschild + χ + Q

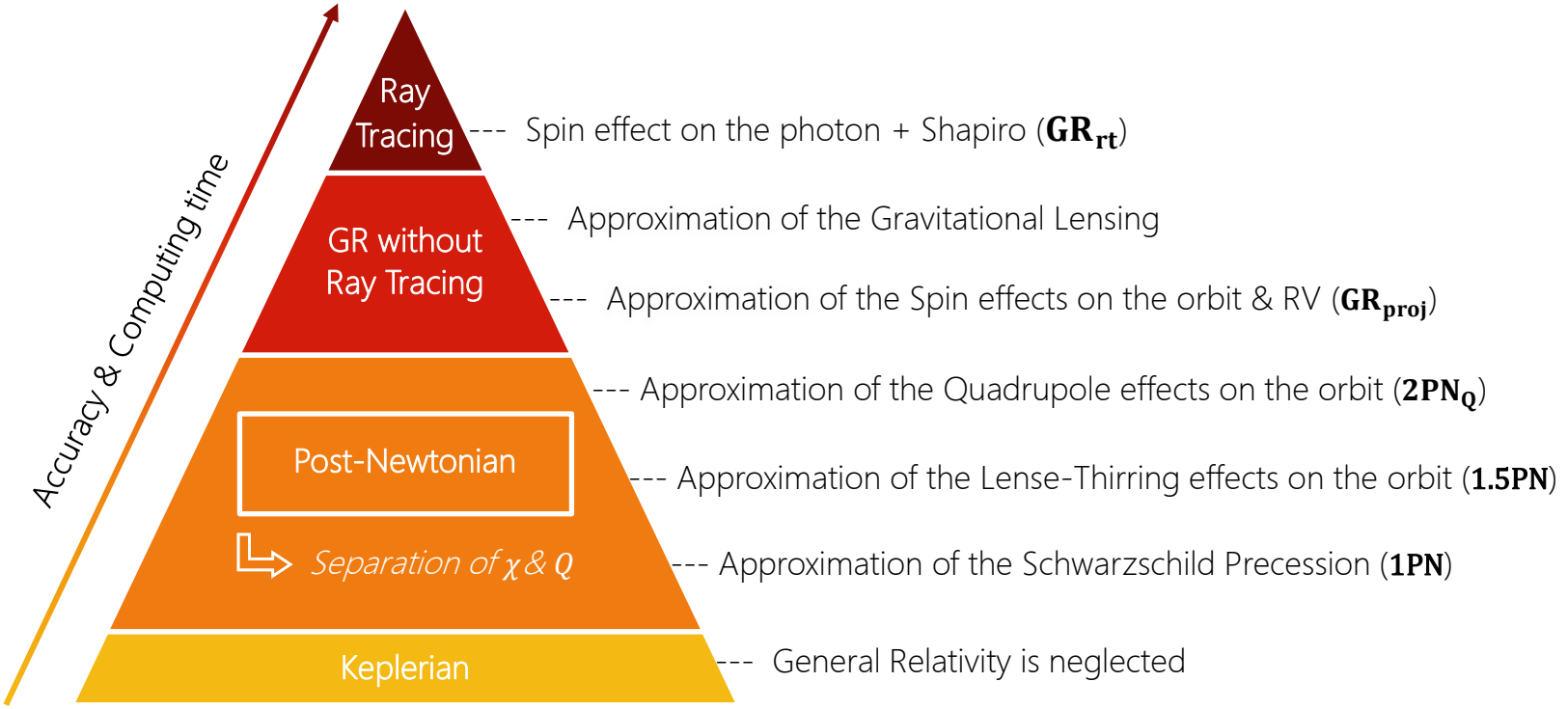

Development of the **1.5PN**, $\mathbf{GR_{proj}}$ and $\mathbf{2PN_Q}$ models

Karim

Studying the secular shift of orbital parameters

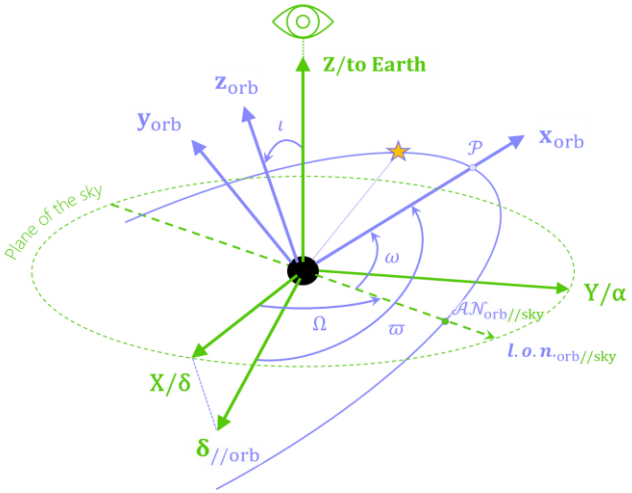

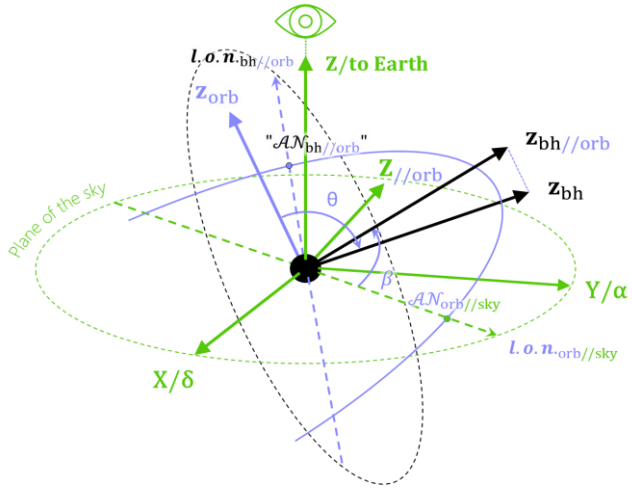

2 TYPES OF PRECESSIONS AT THE 2PN ORDER

- IN-PLANE PRECESSION:
  - Around $\mathbf{z_{orb}}$
  - Due to:
    - Schwarzschild
    - χ
    - Q

Studying the secular shift of orbital parameters

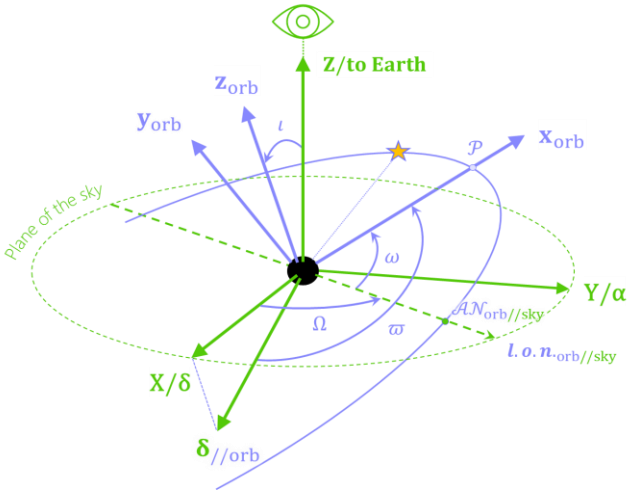

2 TYPES OF PRECESSIONS AT THE 2PN ORDER

- IN-PLANE PRECESSION:
  - Around $\mathbf{z_{orb}}$
  - Due to:
    - Schwarzschild
    - χ
    - Q

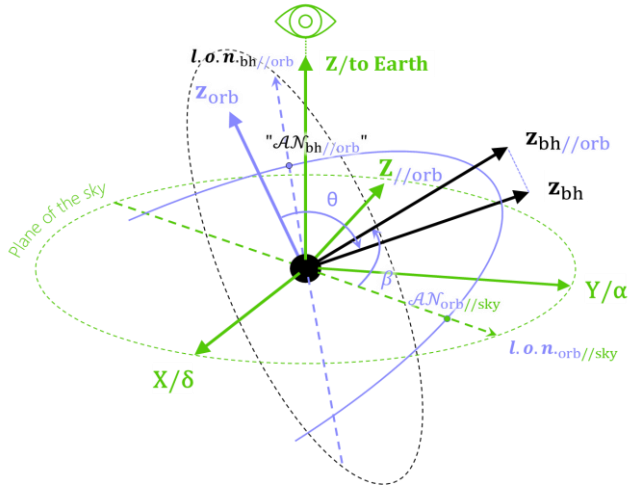

- OUT-OF-PLANE PRECESSION:
  - Around $\mathbf{z_{bh}}$ at fixed θ
  - Due to:
    - χ
    - Q

Studying the secular shift of orbital parameters

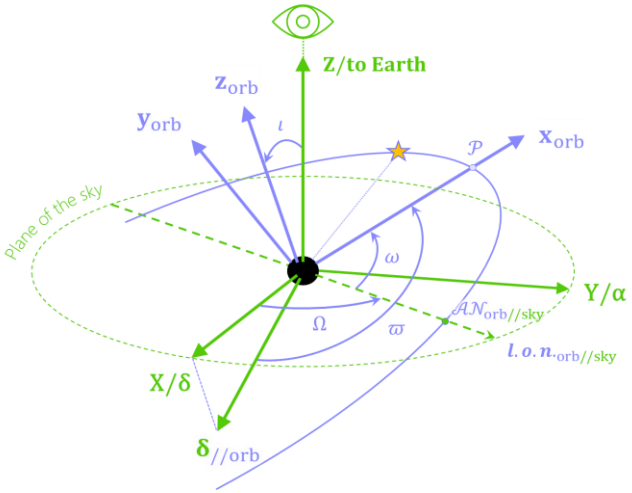

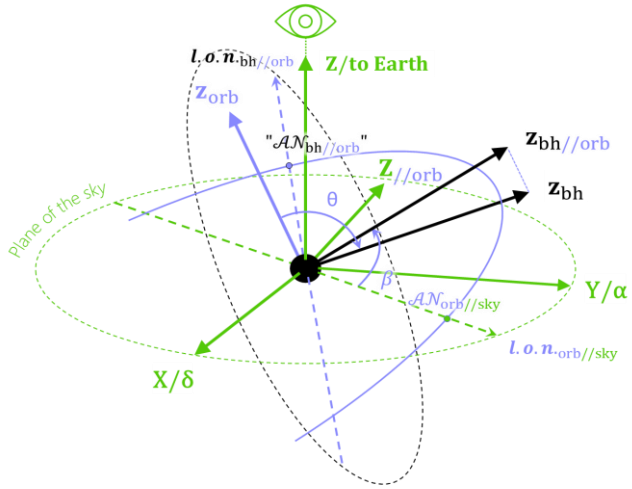

2 TYPES OF PRECESSIONS AT THE 2PN ORDER

❑ IN-PLANE PRECESSION:

- Around $\mathbf{z_{orb}}$
- Due to:
  - Schwarzschild
  - χ
  - Q
- Characterised by:
  $\Delta\varpi = \Delta\omega + cos\iota\Delta\Omega$

❑ OUT-OF-PLANE PRECESSION:

- Around $\mathbf{z_{bh}}$ at fixed θ
- Due to:
  - χ
  - Q
- Characterised by:
  $\Delta\Theta = sin\omega\Delta\iota - cos\omega sin\iota\Delta\Omega$

Independent of the observer !

Studying the secular shift of orbital parameters

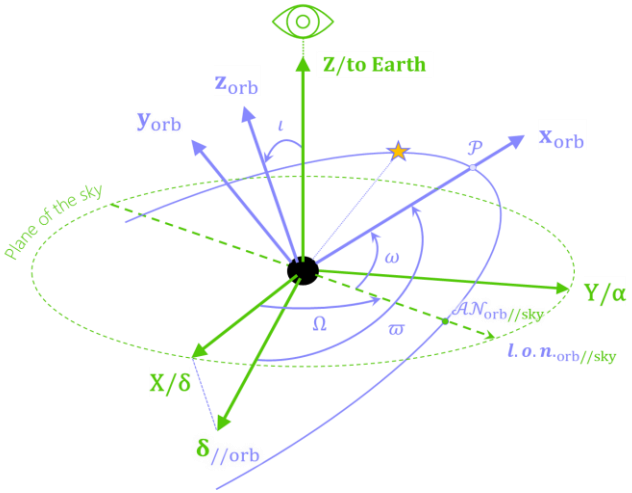

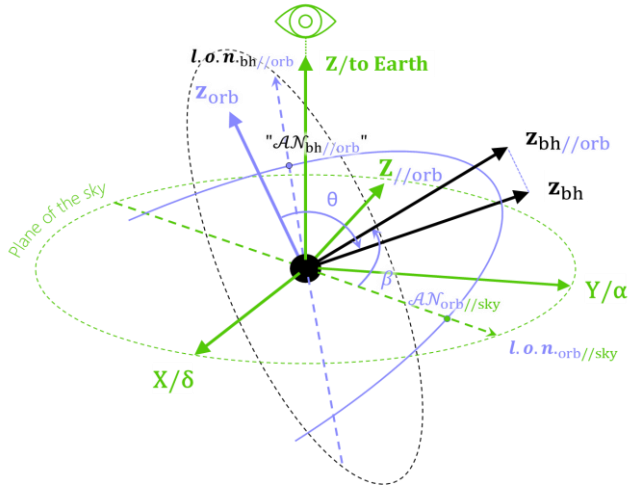

2 TYPES OF PRECESSIONS AT THE 2PN ORDER

❑ IN-PLANE PRECESSION:

- Around $\mathbf{z_{orb}}$
- Due to:
  - Schwarzschild
  - χ
  - Q
- Characterised by:
  $\Delta\varpi = \Delta\omega + cos\iota\Delta\Omega$

❑ OUT-OF-PLANE PRECESSION:

- Around $\mathbf{z_{bh}}$ at fixed θ
- Due to:
  - χ
  - Q
- Characterised by:
  $\Delta\Theta = sin\omega\Delta\iota - cos\omega sin\iota\Delta\Omega$

ANALYTICAL EXPRESSION OF THE SECULAR SHIFT OF ORBITAL PARAMETERS:

$$\Delta\varpi_{\rm Sch} = \Delta\omega_{\rm Sch} = \frac{6\pi Gm}{c^2 p} + \frac{\pi G^2 m^2}{2c^4 p^2}(28 - e^2)$$

$$\Delta\varpi_{\chi} = -\frac{8\pi}{c^3}\left[\frac{Gm}{p}\right]^{3/2}\cos\theta\,\chi$$

$$\Delta\varpi_{Q} = \frac{3\pi}{2c^4}\left[\frac{Gm}{p}\right]^{2}\left(1 - 3\cos^2\theta\right)\chi^2$$

↳ Maximal for $\theta = 0$: an orbit in the equatorial plane of the BH

$$\Delta\Theta_{\chi} = \frac{4\pi}{c^3}\left[\frac{Gm}{p}\right]^{3/2}\sin\theta\sin(\omega - \beta)\;\chi$$

$$\Delta\Theta_{Q} = \frac{3\pi}{c^4}\left[\frac{Gm}{p}\right]^{2}\cos\theta\sin\theta\sin(\omega - \beta)\;\chi^2$$

↳ Null for $\theta = 0$: an orbit in the equatorial plane of the BH

Studying the secular shift of orbital parameters

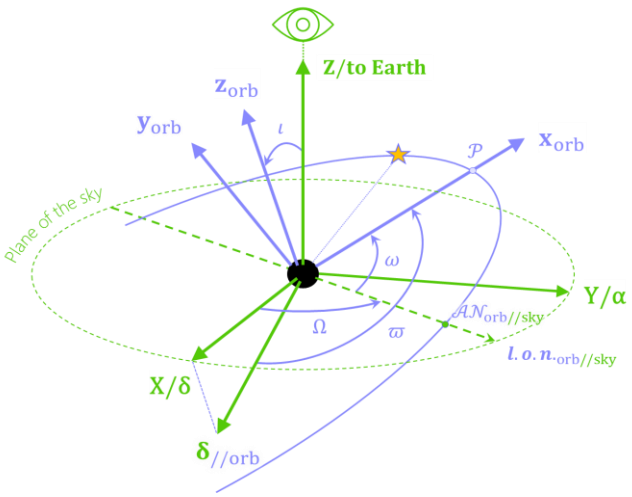

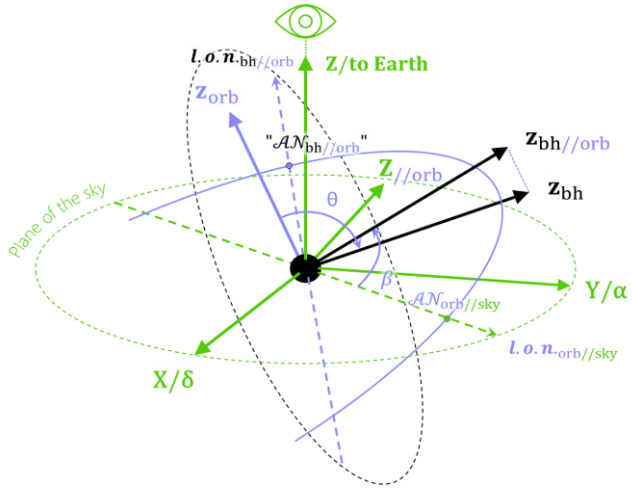

- IN-PLANE PRECESSION:
  - Around z_{orb}
  - Due to:
    - Schwarzschild
    - χ
    - Q
  - Characterised by: $\Delta\varpi = \Delta\omega + cos\iota\Delta\Omega$

ANALYTICAL EXPRESSION OF THE SECULAR SHIFT OF ORBITAL PARAMETERS:

$$\Delta\varpi_{Sch} = \Delta\omega_{Sch} = \frac{6\pi Gm}{c^2 p} + \frac{\pi G^2 m^2}{2c^4 p^2}(28 - e^2)$$

$$\Delta\varpi_{\chi} = -\frac{8\pi}{c^3}\left[\frac{Gm}{p}\right]^{3/2}\cos\theta\,\chi$$

$$\Delta\varpi_{Q} = \frac{3\pi}{2c^4}\left[\frac{Gm}{p}\right]^{2}\left(1 - 3\cos^2\theta\right)\chi^2$$

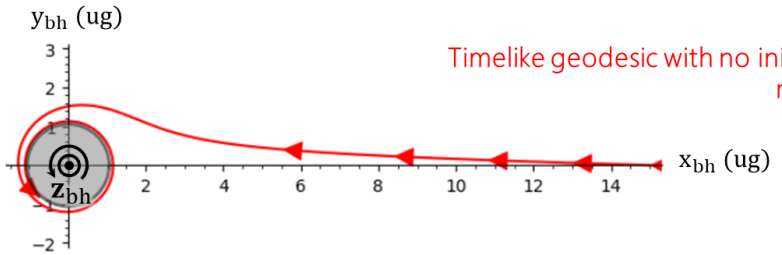

Timelike geodesic with no initial angular momentum

[Adapted from Eric's Gourgoulhon Lecture notes]

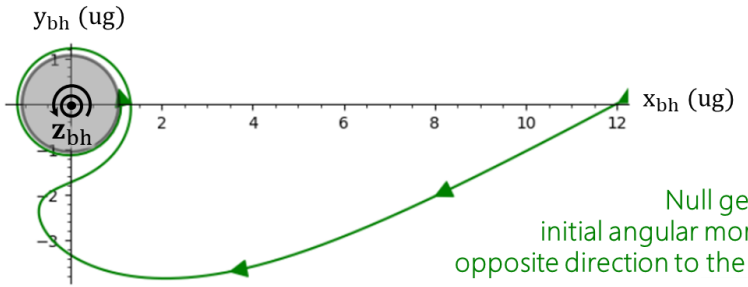

Null geodesic with an initial angular momentum in the opposite direction to the spin of the BH

Studying the secular shift of orbital parameters

Hypothetical star with considerable relativistic effects:

Name	"Ecc"
Period	0.38696 yr
Eccentricity	0.99

SIMULATION WITH 3 CODE MODELS:

2PN_sch : Schwarzschild

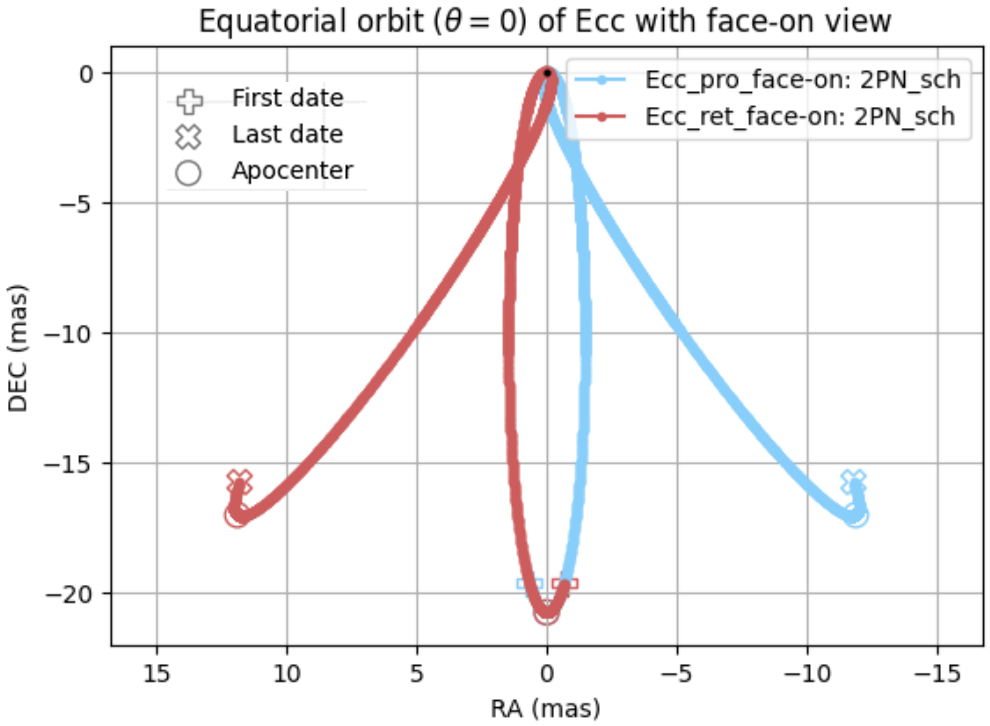

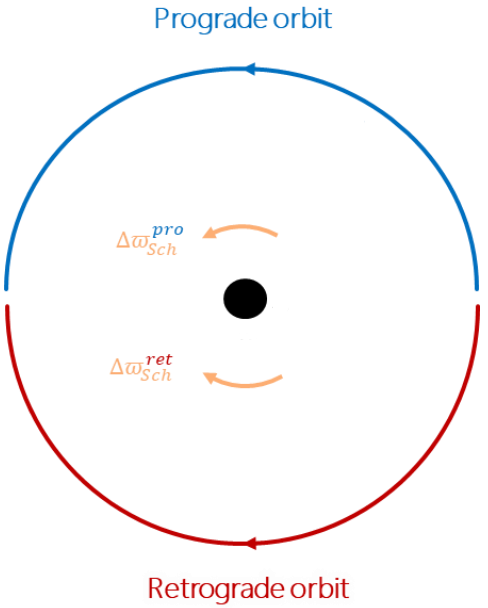

Studying the secular shift of orbital parameters

WHAT HAPPENS WHEN WE ADD A BH SPIN IN THE SAME PLANE ?

SIMULATION WITH 3 CODE MODELS:

2PN_sch : Schwarzschild

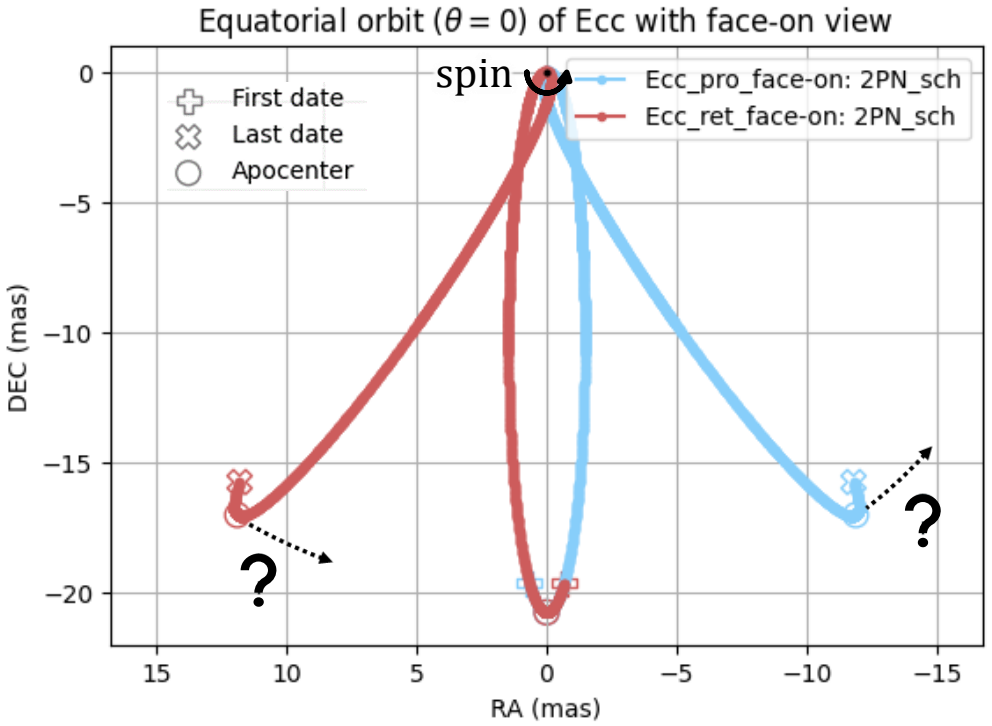

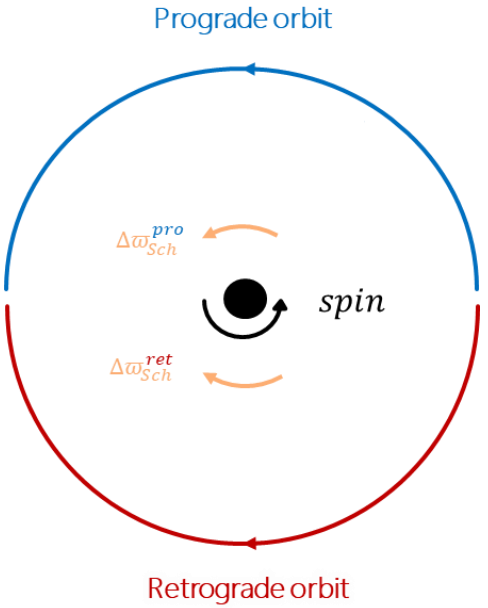

Studying the secular shift of orbital parameters

⚠ Secular shift opposes the spin

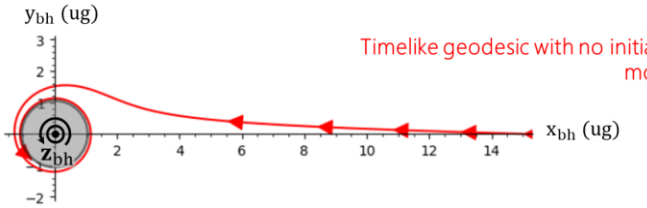

Timelike geodesic with no initial angular momentum

[Adapted from Eric's Gourgoulhon Lecture notes]

SIMULATION WITH 3 CODE MODELS:

2PN_sch : Schwarzschild

2PN_LT : Schwarzschild + χ

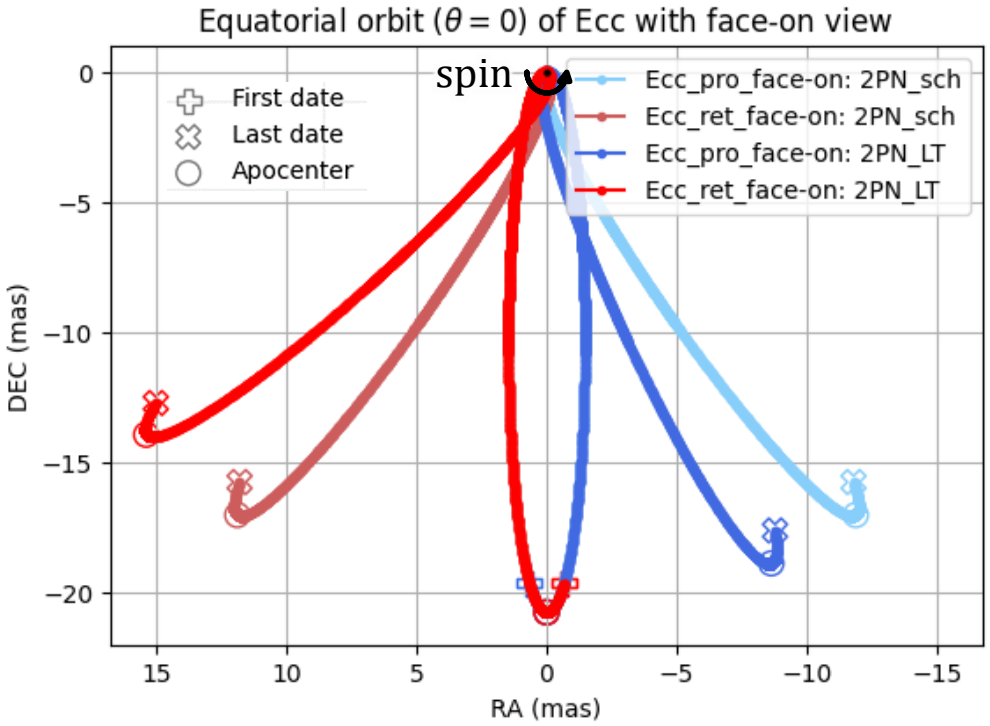

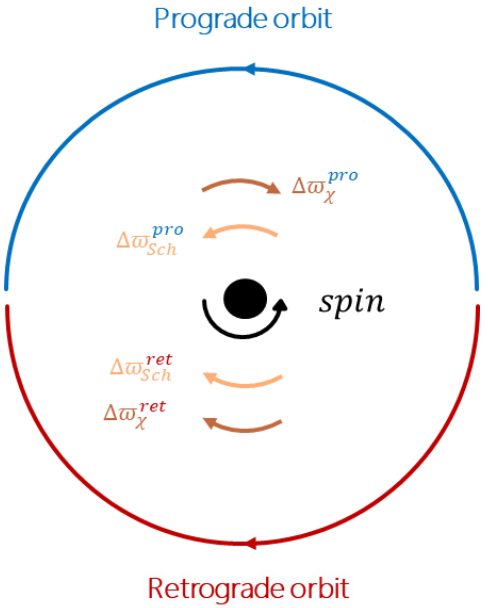

Studying the secular shift of orbital parameters

⚠ Secular shift opposes the spin

⚠ In simulations: $\Delta\varpi_{\chi}^{pro} \neq \Delta\varpi_{\chi}^{ret}$

SIMULATION WITH 3 CODE MODELS:

2PN_sch : Schwarzschild

2PN_LT : Schwarzschild + χ

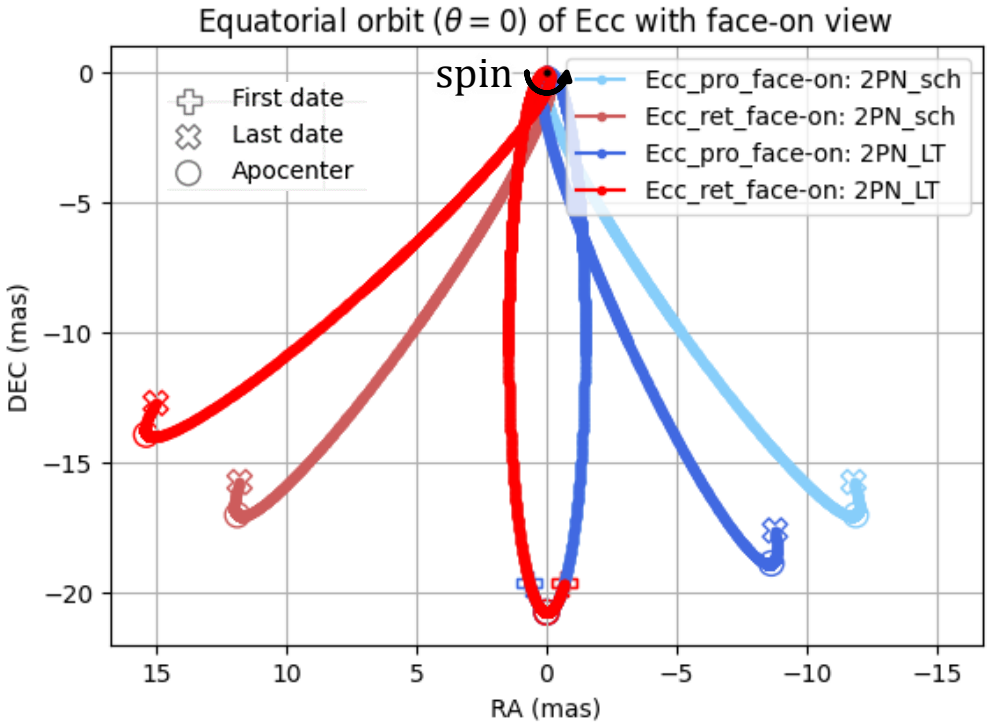

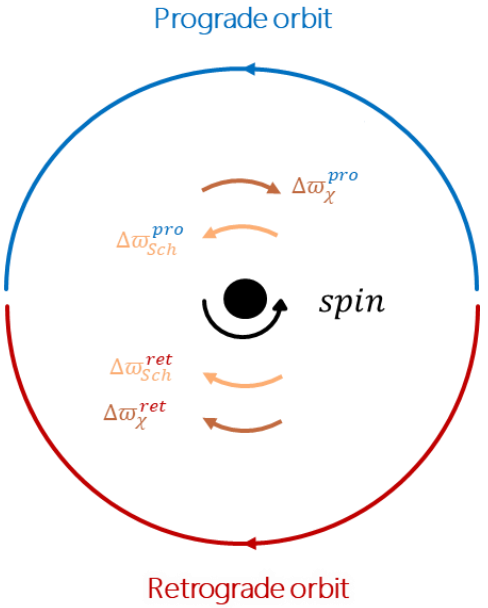

Studying the secular shift of orbital parameters

⚠ Secular shift opposes the spin

⚠ In simulations:
$\Delta\varpi_{\chi}^{pro} \neq \Delta\varpi_{\chi}^{ret}$ & $\Delta\varpi_{Q}^{pro} \neq \Delta\varpi_{Q}^{ret}$

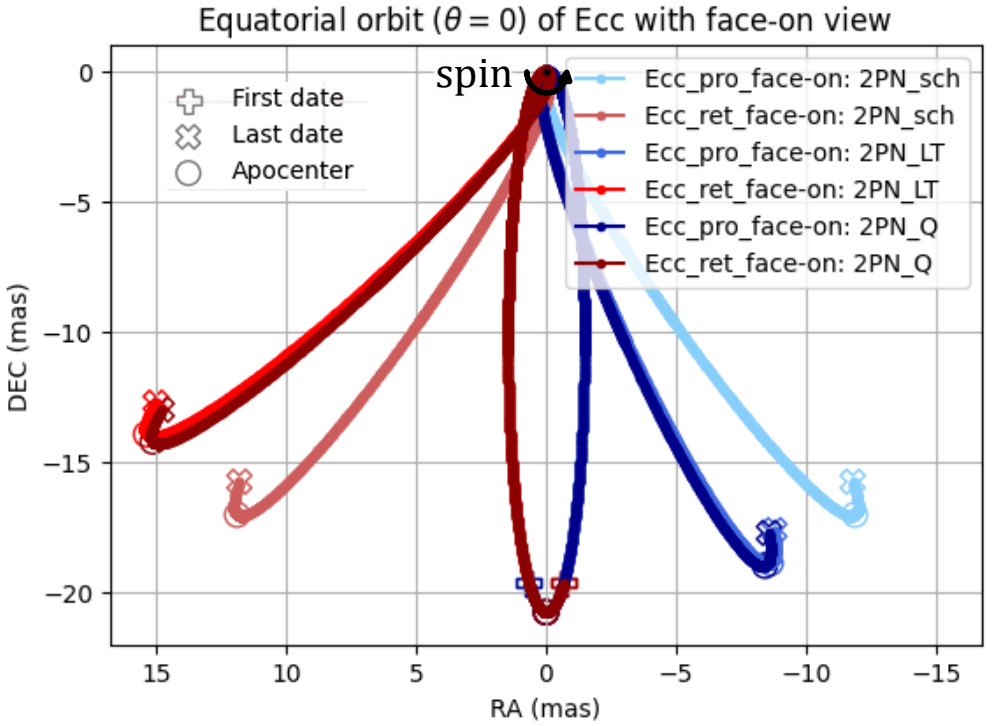

SIMULATION WITH 3 CODE MODELS:

2PN_sch : Schwarzschild

2PN_LT : Schwarzschild + χ

2PN_Q : Schwarzschild + χ + Q

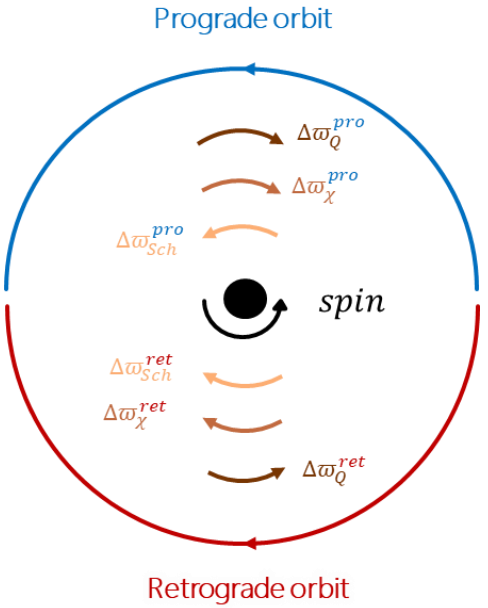

In-plane precession

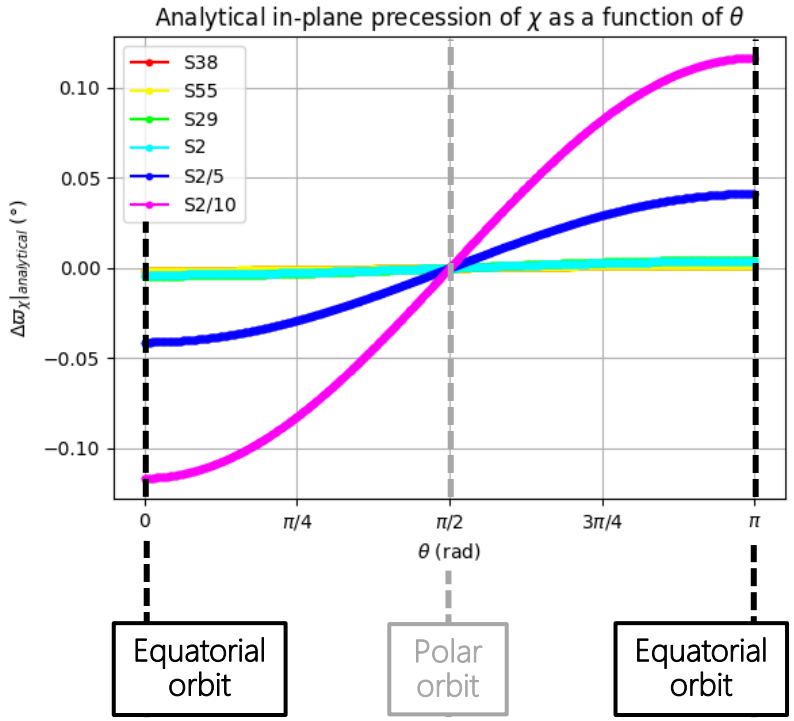

Out-of-plane precession

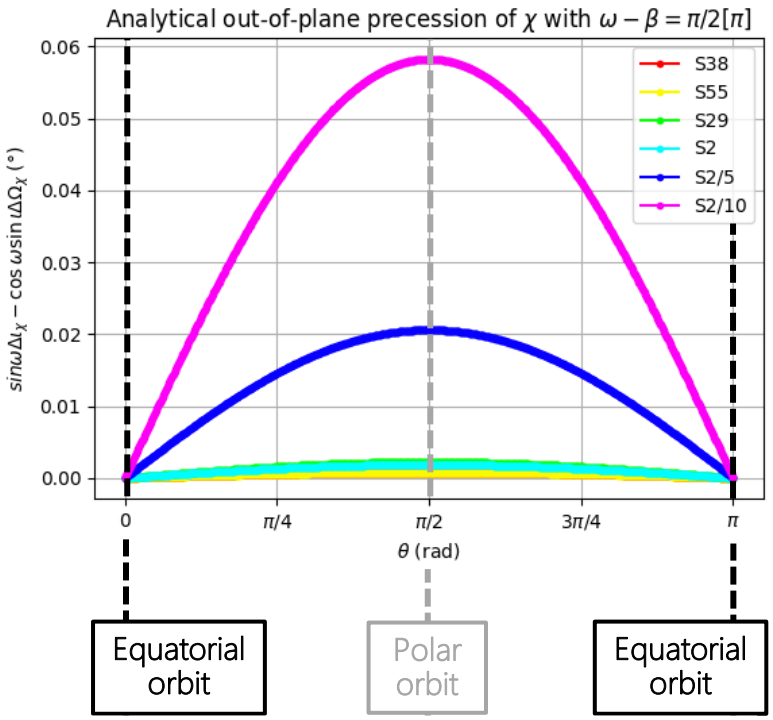

In-plane precession

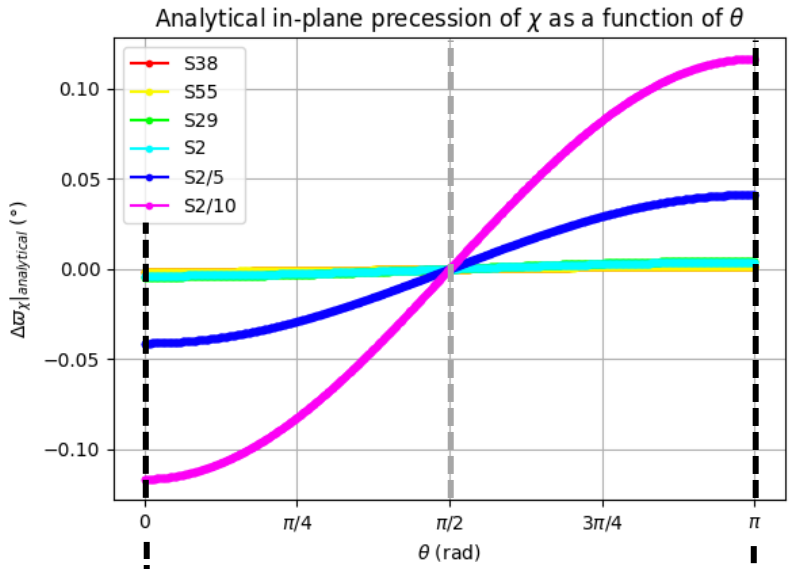

Equatorial orbit

Polar orbit

Equatorial orbit

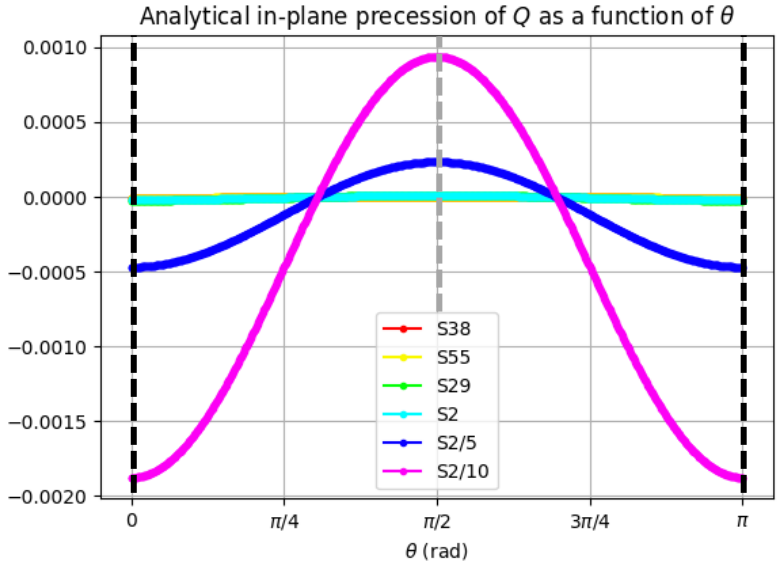

Out-of-plane precession

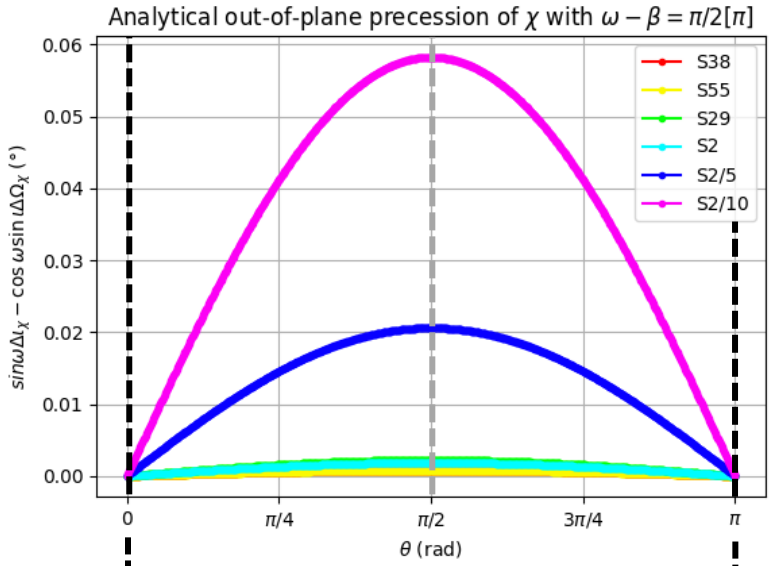

Equatorial orbit

Polar orbit

Equatorial orbit

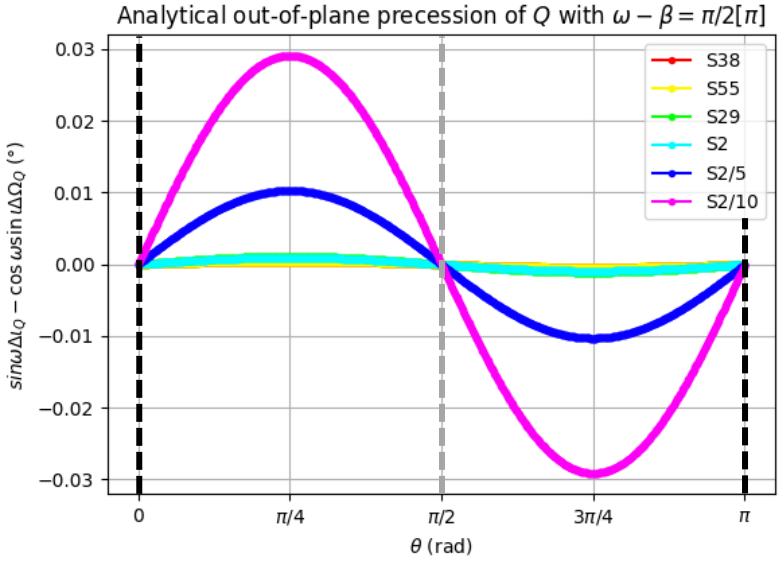

Astronomy & Astrophysics manuscript no. output
May 16, 2024

Sgr A*'s spin and quadrupole moment effects on the orbits of S stars

K. Abd El Dayem[1], G. Heissel[1,2], F. Vincent[1], T. Paumard[1], and G. Perrin[1]

[1] LESIA, Observatoire de Paris, Université PSL, CNRS, Sorbonne Université, Université Paris Cité, 5 place Jules Janssen, 92195 Meudon, France
e-mail: karim.abdeldayem@obspm.fr
[2] Advanced Concepts Team, European Space Agency, TEC-SF, ES-TEC, Keplerlaan 1, NL-2201, AZ Noordwijk, The Netherlands

Received December ?, 2023; accepted ?, 2024

ABSTRACT

Context. Measuring the astrometric and spectroscopic data of stars orbiting the central black hole in our galaxy (Sgr A*) offer a promising way to measure relativistic effects. In principle, the "no-hair" theorem can be tested at the Galactic Center by monitoring the orbital precession of S-stars due to the angular momentum (or spin) and quadrupole moment of Sgr A*.
Aims. In this paper we investigate what stellar orbit and spin orientation are needed to measure the spin and quadrupole moment of Sgr A*. This, allows us to study the detectability of these quantities enabling the testing of the "no-hair" theorem and thus of general relativity (GR).
Methods. We consider a collection of S stars as well as a putative stars that orbit closer to Sgr A*, thus being much more affected by the spin and quadrupole effects. It is possible that either future observations of GRAVITY+ could detect such inner stars that might have been too faint to be detected by GRAVITY. To reach our objectives, we use different relativistic models in order to generate the orbit and radial velocity of the putative stars and analyze how their precession can be affected by the relative orientations of the spin, the orbits and the observer.
Results.

Key words. black hole physics – gravitation – Galaxy: center – relativistic processes - techniques: interferometric

1. Introduction

After years of monitoring S stars in the central parsec of the Milky Way studies have demonstrated the presence of a supermassive black hole (SMBH) called Sgr A* at the center of the Galaxy (Eckart & Genzel 1996; Ghez et al. 1998, 2003, 2008; Schödel et al. 2002; Gillessen et al. 2009, 2017; GRAVITY Collaboration et al. 2022a). According to the "no-hair" theorem, a black hole can be completely characterized by only three externally observable classical parameters: mass, angular momentum (hereafter referred to as spin), and electric charge which will be set to zero in our study. If we consider in addition the quadrupole moment, it must be linked to the mass and spin according to the no-hair theorem. Thus, the latter can be tested by independently measuring these 3 quantities. Dozens of S star orbits are currently known (Gillessen et al. 2017), including the highly elliptical one of the star S2 with a 16 year period, reaching $R \approx 1300 R_S \approx 120$AU from Sgr A* at its pericenter, where $R_S = 2\frac{GM_\bullet}{c^2}$ with G and $M_\bullet$ being the gravitational constant and the black hole's mass respectively. By combining the infrared light collected by the 4 Unit Telescopes of the Very Large Telescope (VLT) at Paranal, the interferometric instrument GRAVITY (General Relativity Analysis via VIt InTerferometrY) was able to estimate the mass of Sgr A* at $M_\bullet \approx 4.297\ 10^6 M_\odot$. Even-though the spin and quadrupole moment of the black hole are still unknown, the future monitoring of S stars could, in principle, provide constraints on these parameters (Will 2008; Angélil & Saha 2014; Alush & Stone 2022) which in turn would allow us to test the "no-hair" theorem.

The different relativistic effects that can be observed in the vicinity of a strong gravitational field like the one surrounding Sgr A* can be divided into 2 categories. The Schwarzschild effects in the case of a non-rotating black hole:

- The Schwarzschild precession which is due to the spacetime curvature on the star trajectory. The orbit precesses because of the gravitational field caused by the central mass (Sgr A* for instance). Thus, the pericenter and apocenter of the star are shifted from one period to another. This affects both the astrometry and the spectroscopy.
- The Shapiro time delay which is due to the slowdown of the proper time of the photon with respect to the proper time of the observer when the photon crosses a gravitational field. This affects both the astrometry and the spectroscopy.
- The relativistic redshifts which can be decomposed into two components. The transversal Doppler shift appears in special relativity and is due to the relative motion between the emitter and the observer. The gravitational redshift appears in GR and is due to the spacetime curvature. This only affects the spectroscopy.
- The gravitational lensing effect which is due to the curvature of the photon geodesic (including spin effects on the photon trajectory) that changes the apparent position of the star on the sky plane. This affects both the astrometry and the spectroscopy.
- Relativistic aberration is the relativistic version of the aberration of light. This affects both the astrometry and the spectroscopy

- Wrap up 1st paper:

  Abd El Dayem et al. 2024

- Get back to the analysis of the detectability of the spin using multiple stars

- Write 2nd paper about multi-star fits

Orbit fitting for spin detectability

Acomplished Work

Development of the **1.5PN**, $\mathbf{GR_{proj}}$ & $\mathbf{2PN_Q}$ models

Analytical expression of secular effects to 2PN

Confrontation of the results in KerrKS and KerrBL

Thank you for your attention

Galactic center and the effects produced by Sgr A*

Astrometry and spectroscopy

Acquired Knowledge

Relativistic dynamics and use of different metrics

Intuition on the impact of the relative orientations

1st Year work:

- Spin effects on other S stars
- Coordinate system effects
- Orbit fitting of spin angles

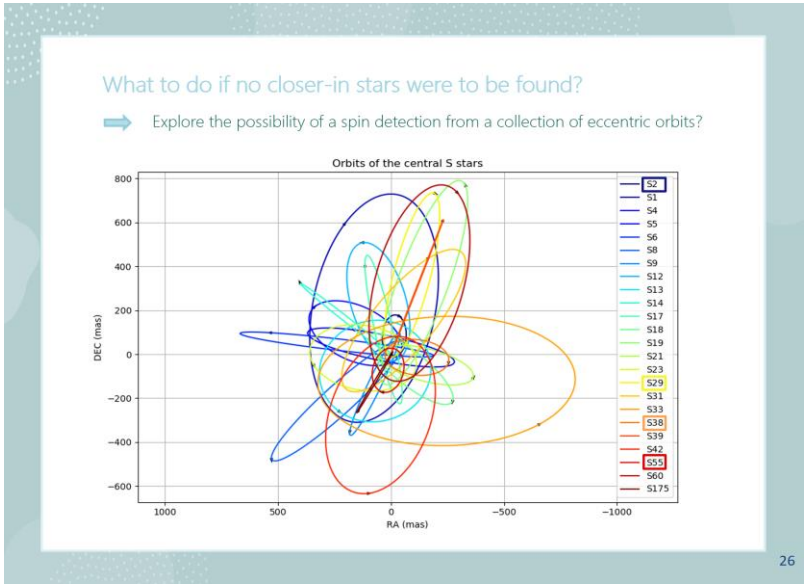

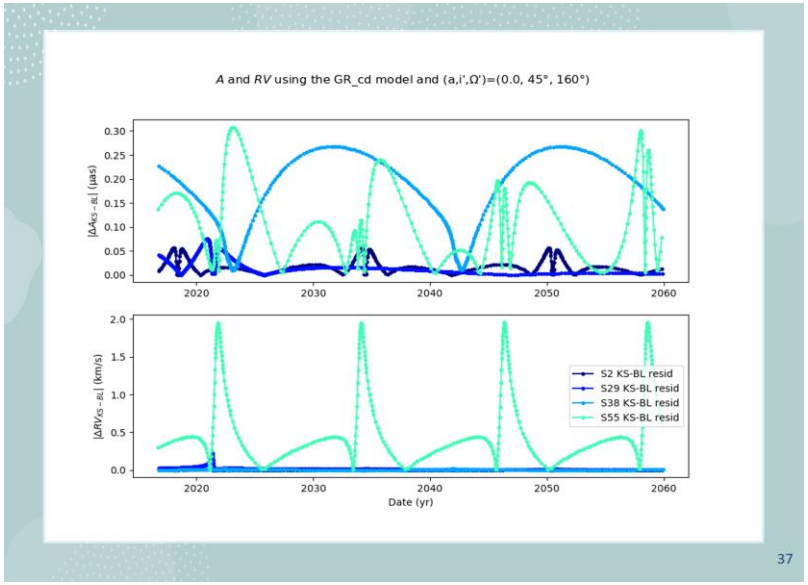

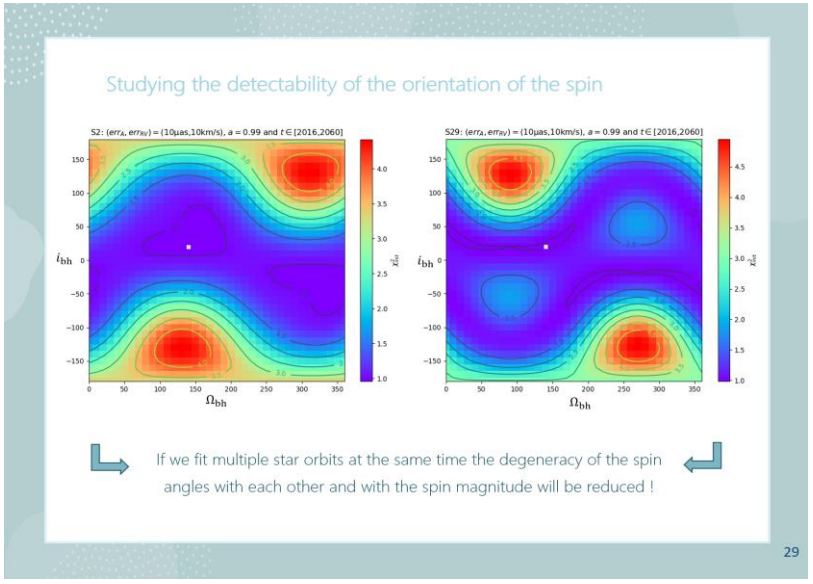

Comparing PN simulations & analytical expression

2 approximations not in the simulations:

$$\frac{d\mu}{df} = \frac{d\mu}{dt}\frac{dt}{df} = F^{\mu}(f, p(f), e(f), \beta(f))$$

A1

$$\frac{dt}{df} = \sqrt{\frac{p^3}{Gm}}\frac{1}{(1+e\cos f)^2}\left[1 + \Psi + \Psi^2 + \Psi^3 + \ldots\right] \longrightarrow \boxed{\frac{dt}{df} \approx \sqrt{\frac{p^3}{Gm}}\frac{1}{(1+e\cos f)^2}}$$

with:

$$\Psi = F^{\Psi}(p, e, \beta, f) \ll 1$$

$$\Psi_{\mathrm{Sch}} = O\left(\frac{v^2}{c^2}\right);\ \Psi_{\chi} = O\left(\frac{v^3}{c^3}\right);\ \Psi_{Q} = O\left(\frac{v^4}{c^4}\right)$$

A2 When integrating the infenitesimal expression of a parameter over f, the other parameters are constants of f

$$\Delta\mu = \int_{f_0}^{f_0+2\pi} F^{\mu}(f, p(f), e(f), \beta(f))\, df$$

$$\approx \mathcal{F}^{\mu}(p, e, \beta)$$

A1

$$\frac{dt}{df} \approx \sqrt{\frac{p^3}{Gm}} \frac{1}{(1+e\cos f)^2}$$

VS

A1′

$$\frac{dt}{df} \approx \sqrt{\frac{p^3}{Gm}} \frac{1}{(1+e\cos f)^2} [1+\Psi]$$

$$\Psi = -\frac{1}{e}\frac{p^2}{Gm}\left(\frac{\cos f}{(1+e\cos f)^2}\mathcal{S} - \frac{2+e\cos f}{(1+e\cos f)^3}\sin f\mathcal{T}\right)$$

$$\Delta\varpi_{\rm Sch} = \int_{f_0}^{f_0+2\pi} \frac{d\varpi_{\rm Sch}}{df}\, df$$
$$= \frac{6\pi Gm}{c^2 p} + \frac{\pi G^2 m^2}{2c^4 p^2}(28-e^2)$$

VS

$$\Delta\varpi_{\rm Sch} = \int_{f_0}^{f_0+2\pi} \frac{d\varpi_{\rm Sch}}{df}\, df$$
$$= \frac{6\pi Gm}{c^2 p} + \frac{\pi G^2 m^2}{2c^4 p^2}\left(\frac{9}{e^2}+51+\frac{e^2}{2}\right) + \frac{\pi G^3 m^3}{2e^2 c^6 p^3}\left(-108-79e^2+15e^4\right)$$
$$= \frac{6\pi Gm}{c^2 p} + \frac{\pi G^2 m^2}{2c^4 p^2}\left(\frac{9}{e^2}+51+\frac{e^2}{2}\right) + \mathcal{O}\left(\frac{v^6}{c^6}\right)$$

$$\Delta\varpi_{\chi} = \int_{f_0}^{f_0+2\pi} \frac{d\varpi_{\chi}}{df}\, df$$
$$= -\frac{8\pi}{c^3}\left[\frac{Gm}{p}\right]^{3/2}\cos\theta\,\chi$$

VS

$$\Delta\varpi_{\chi} = \int_{f_0}^{f_0+2\pi} \frac{d\varpi_{\chi}}{df}\, df$$
$$= -\frac{8\pi}{c^3}\left[\frac{Gm}{p}\right]^{3/2}\cos\theta\,\chi + \frac{4\pi}{e^2}\frac{(Gm)^3}{c^6 p^3}(1+10e^2+e^4)\cos^2\theta\,\chi^2$$
$$= -\frac{8\pi}{c^3}\left[\frac{Gm}{p}\right]^{3/2}\cos\theta\,\chi + \mathcal{O}\left(\frac{v^6}{c^6}\right)$$

$$\Delta\varpi_{Q} = \int_{f_0}^{f_0+2\pi} \frac{d\varpi_{Q}}{df}\, df$$
$$= \frac{3\pi}{2c^4}\left[\frac{Gm}{p}\right]^2\left(1-3\cos^2\theta\right)\chi^2$$

VS

$$\Delta\varpi_{Q} = \int_{f_0}^{f_0+2\pi} \frac{d\varpi_{Q}}{df}\, df$$
$$= \frac{3\pi}{2c^4}\left[\frac{Gm}{p}\right]^2\left(1-3\cos^2\theta\right)\chi^2 + \frac{G^4m^4}{c^8p^4}\chi^4[\ldots]$$
$$= \frac{3\pi}{2c^4}\left[\frac{Gm}{p}\right]^2\left(1-3\cos^2\theta\right)\chi^2 + \mathcal{O}\left(\frac{v^8}{c^8}\right)$$

A1 $\frac{dt}{df} \approx \sqrt{\frac{p^3}{Gm}} \frac{1}{(1+e\cos f)^2}$

VS

A1′ $\frac{dt}{df} \approx \sqrt{\frac{p^3}{Gm}} \frac{1}{(1+e\cos f)^2} [1+\Psi]$

$$\Psi = -\frac{1}{e}\frac{p^2}{Gm}\left(\frac{\cos f}{(1+e\cos f)^2}\mathcal{S} - \frac{2+e\cos f}{(1+e\cos f)^3}\sin f\mathcal{T}\right)$$

$$\Delta\varpi_{\rm Sch} = \int_{f_0}^{f_0+2\pi} \frac{d\varpi_{\rm Sch}}{df} df$$
$$= \frac{6\pi Gm}{c^2 p} + \frac{\pi G^2 m^2}{2c^4 p^2}(28 - e^2)$$

A1′ **is more precise even at** $\mathcal{O}\left(\frac{v^4}{c^4}\right)$

$$\Delta\varpi_{\rm Sch} = \int_{f_0}^{f_0+2\pi} \frac{d\varpi_{\rm Sch}}{df} df$$
$$= \frac{6\pi Gm}{c^2 p} + \frac{\pi G^2 m^2}{2c^4 p^2}\left(\frac{9}{e^2} + 51 + \frac{e^2}{2}\right) + \frac{\pi G^3 m^3}{2e^2 c^6 p^3}\left(-108 - 79e^2 + 15e^4\right)$$
$$= \frac{6\pi Gm}{c^2 p} + \frac{\pi G^2 m^2}{2c^4 p^2}\left(\frac{9}{e^2} + 51 + \frac{e^2}{2}\right) + \mathcal{O}\left(\frac{v^6}{c^6}\right)$$

$$\Delta\varpi_\chi = \int_{f_0}^{f_0+2\pi} \frac{d\varpi_\chi}{df} df$$
$$= -\frac{8\pi}{c^3}\left[\frac{Gm}{p}\right]^{3/2}\cos\theta\,\chi$$

VS

$$\Delta\varpi_\chi = \int_{f_0}^{f_0+2\pi} \frac{d\varpi_\chi}{df} df$$
$$= -\frac{8\pi}{c^3}\left[\frac{Gm}{p}\right]^{3/2}\cos\theta\,\chi + \frac{4\pi}{e^2}\frac{(Gm)^3}{c^6 p^3}(1+10e^2+e^4)\cos^2\theta\chi^2$$
$$= -\frac{8\pi}{c^3}\left[\frac{Gm}{p}\right]^{3/2}\cos\theta\,\chi + \mathcal{O}\left(\frac{v^6}{c^6}\right)$$

$$\Delta\varpi_Q = \int_{f_0}^{f_0+2\pi} \frac{d\varpi_Q}{df} df$$
$$= \frac{3\pi}{2c^4}\left[\frac{Gm}{p}\right]^2\left(1-3\cos^2\theta\right)\chi^2$$

VS

$$\Delta\varpi_Q = \int_{f_0}^{f_0+2\pi} \frac{d\varpi_Q}{df} df$$
$$= \frac{3\pi}{2c^4}\left[\frac{Gm}{p}\right]^2\left(1-3\cos^2\theta\right)\chi^2 + \frac{G^4m^4}{c^8p^4}\chi^4[\ldots]$$
$$= \frac{3\pi}{2c^4}\left[\frac{Gm}{p}\right]^2\left(1-3\cos^2\theta\right)\chi^2 + \mathcal{O}\left(\frac{v^8}{c^8}\right)$$

A1 $\frac{dt}{df} \approx \sqrt{\frac{p^3}{Gm}} \frac{1}{(1+e\cos f)^2}$

VS

A1′ $\frac{dt}{df} \approx \sqrt{\frac{p^3}{Gm}} \frac{1}{(1+e\cos f)^2} [1+\Psi]$

$$\Psi = -\frac{1}{e}\frac{p^2}{Gm}\left(\frac{\cos f}{(1+e\cos f)^2}\mathcal{S} - \frac{2+e\cos f}{(1+e\cos f)^3}\sin f\mathcal{T}\right)$$

$$\Delta\varpi_{\rm Sch} = \int_{f_0}^{f_0+2\pi} \frac{d\varpi_{\rm Sch}}{df} df$$

$$= \frac{6\pi Gm}{c^2 p} + \frac{\pi G^2 m^2}{2c^4 p^2}(28 - e^2)$$

A1′ **is more precise even at** $\mathcal{O}\left(\frac{v^4}{c^4}\right)$

$$\Delta\varpi_{\rm Sch} = \int_{f_0}^{f_0+2\pi} \frac{d\varpi_{\rm Sch}}{df} df$$

$$= \frac{6\pi Gm}{c^2 p} + \frac{\pi G^2 m^2}{2c^4 p^2}\left(\frac{9}{e^2} + 51 + \frac{e^2}{2}\right) + \frac{\pi G^3 m^3}{2e^2 c^6 p^3}\left(-108 - 79e^2 + 15e^4\right)$$

$$= \frac{6\pi Gm}{c^2 p} + \frac{\pi G^2 m^2}{2c^4 p^2}\left(\frac{9}{e^2} + 51 + \frac{e^2}{2}\right) + \mathcal{O}\left(\frac{v^6}{c^6}\right)$$

$$\Delta\varpi_\chi = \int_{f_0}^{f_0+2\pi} \frac{d\varpi_\chi}{df} df$$

$$= -\frac{8\pi}{c^3}\left[\frac{Gm}{p}\right]^{3/2} \cos\theta\,\chi$$

Draw

Same at $\mathcal{O}\left(\frac{v^4}{c^4}\right)$

$$\Delta\varpi_\chi = \int_{f_0}^{f_0+2\pi} \frac{d\varpi_\chi}{df} df$$

$$= -\frac{8\pi}{c^3}\left[\frac{Gm}{p}\right]^{3/2} \cos\theta\,\chi + \frac{4\pi}{e^2}\frac{(Gm)^3}{c^6 p^3}(1 + 10e^2 + e^4)\cos^2\theta\chi^2$$

$$= -\frac{8\pi}{c^3}\left[\frac{Gm}{p}\right]^{3/2} \cos\theta\,\chi + \mathcal{O}\left(\frac{v^6}{c^6}\right)$$

$$\Delta\varpi_Q = \int_{f_0}^{f_0+2\pi} \frac{d\varpi_Q}{df} df$$

$$= \frac{3\pi}{2c^4}\left[\frac{Gm}{p}\right]^2 \left(1 - 3\cos^2\theta\right)\chi^2$$

VS

$$\Delta\varpi_Q = \int_{f_0}^{f_0+2\pi} \frac{d\varpi_Q}{df} df$$

$$= \frac{3\pi}{2c^4}\left[\frac{Gm}{p}\right]^2 \left(1 - 3\cos^2\theta\right)\chi^2 + \frac{G^4 m^4}{c^8 p^4}\chi^4[\ldots]$$

$$= \frac{3\pi}{2c^4}\left[\frac{Gm}{p}\right]^2 \left(1 - 3\cos^2\theta\right)\chi^2 + \mathcal{O}\left(\frac{v^8}{c^8}\right)$$

A1

$$\frac{dt}{df} \approx \sqrt{\frac{p^3}{Gm}} \frac{1}{(1+e\cos f)^2}$$

VS

A1′

$$\frac{dt}{df} \approx \sqrt{\frac{p^3}{Gm}} \frac{1}{(1+e\cos f)^2} [1+\Psi]$$

$$\Psi = -\frac{1}{e}\frac{p^2}{Gm}\left(\frac{\cos f}{(1+e\cos f)^2}\mathcal{S} - \frac{2+e\cos f}{(1+e\cos f)^3}\sin f\mathcal{T}\right)$$

$$\Delta\varpi_{\rm Sch} = \int_{f_0}^{f_0+2\pi} \frac{d\varpi_{\rm Sch}}{df} df$$

$$= \frac{6\pi Gm}{c^2 p} + \frac{\pi G^2 m^2}{2c^4 p^2}(28 - e^2)$$

A1′ is more precise even at $\mathcal{O}\left(\frac{v^4}{c^4}\right)$

$$\Delta\varpi_{\rm Sch} = \int_{f_0}^{f_0+2\pi} \frac{d\varpi_{\rm Sch}}{df} df$$

$$= \frac{6\pi Gm}{c^2 p} + \frac{\pi G^2 m^2}{2c^4 p^2}\left(\frac{9}{e^2} + 51 + \frac{e^2}{2}\right) + \frac{\pi G^3 m^3}{2e^2 c^6 p^3}\left(-108 - 79e^2 + 15e^4\right)$$

$$= \frac{6\pi Gm}{c^2 p} + \frac{\pi G^2 m^2}{2c^4 p^2}\left(\frac{9}{e^2} + 51 + \frac{e^2}{2}\right) + \mathcal{O}\left(\frac{v^6}{c^6}\right)$$

$$\Delta\varpi_\chi = \int_{f_0}^{f_0+2\pi} \frac{d\varpi_\chi}{df} df$$

$$= -\frac{8\pi}{c^3}\left[\frac{Gm}{p}\right]^{3/2} \cos\theta\,\chi$$

Draw

Same at $\mathcal{O}\left(\frac{v^4}{c^4}\right)$

$$\Delta\varpi_\chi = \int_{f_0}^{f_0+2\pi} \frac{d\varpi_\chi}{df} df$$

$$= -\frac{8\pi}{c^3}\left[\frac{Gm}{p}\right]^{3/2} \cos\theta\,\chi + \frac{4\pi}{e^2}\frac{(Gm)^3}{c^6 p^3}(1 + 10e^2 + e^4)\cos^2\theta\chi^2$$

$$= -\frac{8\pi}{c^3}\left[\frac{Gm}{p}\right]^{3/2} \cos\theta\,\chi + \mathcal{O}\left(\frac{v^6}{c^6}\right)$$

$$\Delta\varpi_Q = \int_{f_0}^{f_0+2\pi} \frac{d\varpi_Q}{df} df$$

$$= \frac{3\pi}{2c^4}\left[\frac{Gm}{p}\right]^2 \left(1 - 3\cos^2\theta\right)\chi^2$$

Draw

Same at $\mathcal{O}\left(\frac{v^4}{c^4}\right)$

$$\Delta\varpi_Q = \int_{f_0}^{f_0+2\pi} \frac{d\varpi_Q}{df} df$$

$$= \frac{3\pi}{2c^4}\left[\frac{Gm}{p}\right]^2 \left(1 - 3\cos^2\theta\right)\chi^2 + \frac{G^4 m^4}{c^8 p^4}\chi^4[\ldots]$$

$$= \frac{3\pi}{2c^4}\left[\frac{Gm}{p}\right]^2 \left(1 - 3\cos^2\theta\right)\chi^2 + \mathcal{O}\left(\frac{v^8}{c^8}\right)$$

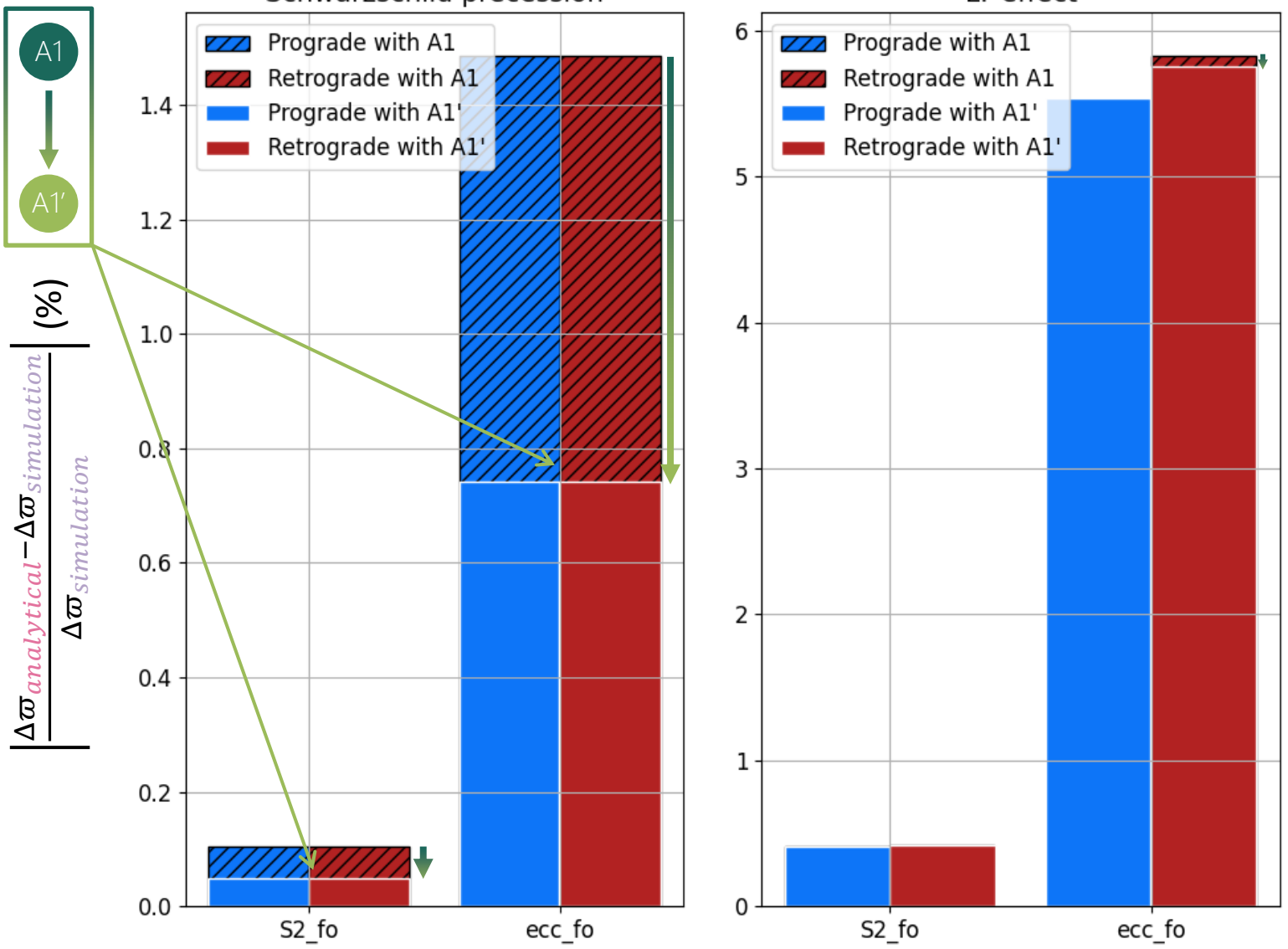
A1
A1′
$\left|\frac{\Delta\varpi_{analytical}-\Delta\varpi_{simulation}}{\Delta\varpi_{simulation}}\right|$ (%)
Schwarzschild precession
Prograde with A1
Retrograde with A1
Prograde with A1'
Retrograde with A1'
0.0
0.2
0.4
0.6
0.8
1.0
1.2
1.4
S2_fo
ecc_fo
LT effect
Prograde with A1
Retrograde with A1
Prograde with A1'
Retrograde with A1'
0
1
2
3
4
5
6
S2_fo
ecc_fo

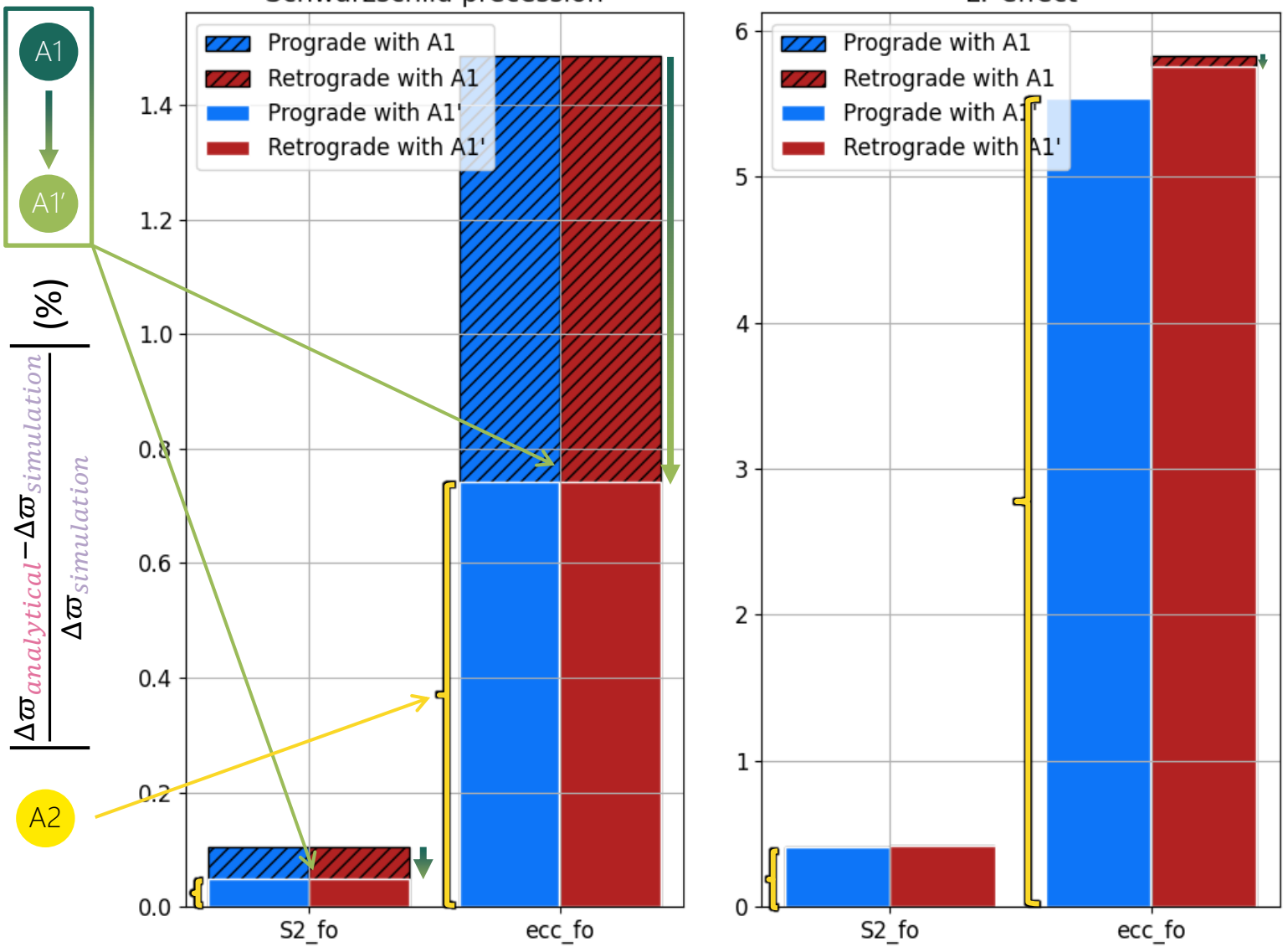
A1
A1′
A2
$\left|\frac{\Delta\varpi_{analytical}-\Delta\varpi_{simulation}}{\Delta\varpi_{simulation}}\right|$ (%)
Schwarzschild precession
Prograde with A1
Retrograde with A1
Prograde with A1'
Retrograde with A1'
0.0
0.2
0.4
0.6
0.8
1.0
1.2
1.4
S2_fo
ecc_fo
LT effect
Prograde with A1
Retrograde with A1
Prograde with A1'
Retrograde with A1'
0
1
2
3
4
5
6
S2_fo
ecc_fo

TAKE HOME MESSAGES

- Using A1′ instead of A1 generates different expression of $\Delta\varpi_{Sch}$ to the 2PN

TAKE HOME MESSAGES

- Using A1′ instead of A1 generates different expression of $\Delta\varpi_{Sch}$ to the 2PN
- PN analytical expressions deviate from the actual PN dynamics mainly due to A2

TAKE HOME MESSAGES

- Using A1′ instead of A1 generates different expression of $\Delta\varpi_{Sch}$ to the 2PN
- PN analytical expressions deviate from the actual PN dynamics mainly due to A2
- Independently of the observer:
  - the $\Delta\varpi_Q$ is maximized for equatorial orbits as well but is still important for polar orbits

TAKE HOME MESSAGES

- Using A1′ instead of A1 generates different expression of $\Delta\varpi_{Sch}$ to the 2PN

- PN analytical expressions deviate from the actual PN dynamics mainly due to A2

- Independently of the observer:
  - ➢ the $\Delta\varpi_Q$ is maximized for equatorial orbits as well but is still important for polar orbits

  - ➢ The $\Delta\Theta$ has 2 types: rotation around major & minor axes

- A face-on view of the orbit maximize $\Delta\varpi$ but minimize $\Delta\Theta$ and edge-on views do the opposite

Cf. Abd El Dayem et al. 2024 (in prep.)

TAKE HOME MESSAGES

- Using A1′ instead of A1 generates different expression of $\Delta\varpi_{Sch}$ to the 2PN
- PN analytical expressions deviate from the actual PN dynamics mainly due to A2
- Independently of the observer:
  - the $\Delta\varpi_Q$ is maximized for equatorial orbits as well but is still important for polar orbits
  - The $\Delta\Theta$ has 2 types: rotation around major & minor axes
- A face-on view of the orbit maximize $\Delta\varpi$ but minimize $\Delta\Theta$ and edge-on views do the opposite